J|A|C|S
ARTICLES
Published on Web 01/04/2003

Role of Copper Ion in Bacterial Copper Amine Oxidase: Spectroscopic and Crystallographic Studies of Metal-Substituted Enzymes

Sei'ichiro Kishishita,[†,§] Toshihide Okajima,[†] Misa Kim,[‡] Hiroshi Yamaguchi,[‡] Shun Hirota,[∥] Shinnichiro Suzuki,[⊥] Shun'ichi Kuroda,[†] Katsuyuki Tanizawa,*[,†] and Minae Mure*[,†,¶]

Contribution from the Institute of Scientific and Industrial Research, Osaka University, Ibaraki, Osaka 567-0047, Japan, Department of Chemistry, School of Science, Kwansei Gakuin University, Nishinomiya, Hyogo 662-8501, Japan, Department of Chemistry, Graduate School of Science, Nagoya University, Chikusa-ku, Nagoya 464-8602, Japan, and Department of Chemistry, Graduate School of Science, Osaka University, Toyonaka, Osaka 560-0043, Japan

Received December 29, 2001; E-mail: mure@eve.cchem.berkeley.edu; tanizawa@sanken.osaka-u.ac.jp

Abstract: The role of the active site Cu^{2+} of phenylethylamine oxidase from *Arthrobacter globiformis* (AGAO) has been studied by substitution with other divalent cations, where we were able to remove >99.5% of Cu^{2+} from the active site. The enzymes reconstituted with Co^{2+} and Ni^{2+} (Co- and Ni-AGAO) exhibited 2.2 and 0.9% activities, respectively, of the original Cu^{2+}-enzyme (Cu-AGAO), but their K_m values for amine substrate and dioxygen were comparable. X-ray crystal structures of the Co- and Ni-AGAO were solved at 2.0−1.8 Å resolution. These structures revealed changes in the metal coordination environment when compared to that of Cu-AGAO. However, the hydrogen-bonding network around the active site involving metal-coordinating and noncoordinating water molecules was preserved. Upon anaerobic mixing of the Cu-, Co-, and Ni-AGAO with amine substrate, the 480 nm absorption band characteristic of the oxidized form of the topaquinone cofactor (TPQ_{ox}) disappeared rapidly (< 6 ms), yielding the aminoresorcinol form of the reduced cofactor (TPQ_{amr}). In contrast to the substrate-reduced Cu-AGAO, the semiquinone radical (TPQ_{sq}) was not detected in Co- and Ni-AGAO. Further, in the latter, TPQ_{amr} reacted reversibly with the product aldehyde to form a species with a λ_{max} at around 350 nm that was assigned as the neutral form of the product Schiff base (TPQ_{pim}). Introduction of dioxygen to the substrate-reduced Co- and Ni-AGAO resulted in the formation of a TPQ-related intermediate absorbing at around 360 nm, which was assigned to the neutral iminoquinone form of the $2e^-$-oxidized cofactor (TPQ_{imq}) and which decayed concomitantly with the generation of TPQ_{ox}. The rate of TPQ_{imq} formation and its subsequent decay in Co- and Ni-AGAO was slow when compared to those of the corresponding reactions in Cu-AGAO. The low catalytic activities of the metal-substituted enzymes are due to the impaired efficiencies of the oxidative half-reaction in the catalytic cycle of amine oxidation. On the basis of these results, we propose that the native Cu^{2+} ion has essential roles such as catalyzing the electron transfer between TPQ_{amr} and dioxygen, in part by providing a binding site for $1e^-$- and $2e^-$-reduced dioxygen species to be efficiently protonated and released and also preventing the back reaction between the product aldehyde and TPQ_{amr}.

Introduction

Copper amine oxidases (EC 1.4.3.6) (CAOs[1]) catalyze the oxidative deamination of various primary amines and occur widely in both prokaryotic and eukaryotic organisms.[2−4] The enzymes are commonly a homodimer of two 70−95 kDa subunits, each containing one copper ion and the redox-active organic cofactor, 2,4,5-trihydroxyphenylalanine quinone or topaquinone (TPQ).[5] It has been well established that the TPQ cofactor is posttranslationally generated by copper-dependent

* Authors to whom correspondence should be addressed.
† Institute of Scientific and Industrial Research, Osaka University.
‡ Kwansei Gakuin University.
∥ Nagoya University. Present address: Kyoto Pharmaceutical University, Yamashina, Kyoto 607-8414, Japan.
⊥ Graduate School of Science, Osaka University.
§ Present address: Protein Research Group, Genomic Sciences Center, RIKEN Yokohama Institute, Yokohama, Kanagawa 230-0045, Japan.
¶ Present address: Department of Chemistry, University of California, Berkeley, CA 94720.

(1) Abbreviations: AGAO, *Arthrobacter globiformis* phenylethylamine oxidase; BSAO, bovine serum amine oxidase; CAO(s), copper amine oxidase(s); Co-AGAO, Co^{2+}-substituted AGAO; Cu_{dep}, Cu^{2+}-depleted; Cu_{rec}, Cu^{2+}-reconstituted; ECAO, *E. coli* amine oxidase; HEPES, *N*-(2-hydroxyethyl)-piperazine-*N*′-(2-ethanesulfonic acid); HPAO, *Hansenula polymorpha* amine oxidase; Ni-AGAO, Ni^{2+}-substituted AGAO; TPQ, 2,4,5-trihydroxyphenylalanine quinone or topaquinone; TPQ_{imq}, iminoquinone form of TPQ; TPQ_{ox}, TPQ in the oxidized form; TPQ_{amr}, aminoresorcinol form of reduced TPQ; TPQ_{red}, trihydroxybenzene form of reduced TPQ; TPQ_{sq}, TPQ semiquinone; TPQ_{pim}, product Schiff base form of TPQ.

(2) McIntire, W. S.; Hartman, C. In *Principles and Applications of Quinoproteins*; Davidson, V. L., Ed.; Marcel Dekker: New York, 1993; pp 97−171.
(3) Klinman, J. P.; Mu, D. *Annu. Rev. Biochem.* **1994**, *63*, 299−344.
(4) Knowles, P. F.; Dooley, D. M. In *Metal Ions in Biological Systems*; Sigel, G., Sigel, A., Eds.; Marcel Dekker: New York, 1994; pp 361−403.

10.1021/ja017899k CCC: $25.00

Scheme 1. Reaction Mechanism of Copper Amine Oxidase

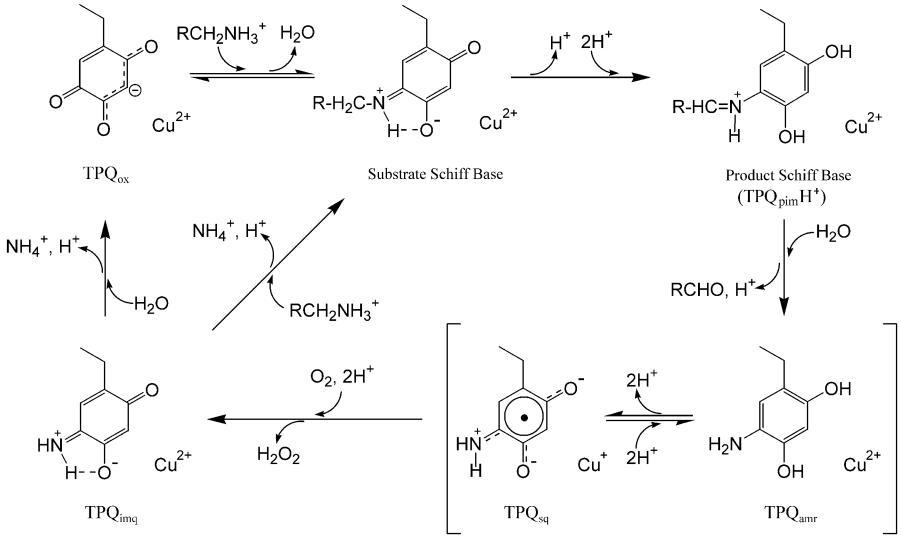

oxidation of a conserved precursor tyrosine residue in the enzyme sequences.[6−9]

The catalytic reaction of CAO proceeds through a ping-pong mechanism, in which the overall reaction can be divided into the initial reductive and the following oxidative half-reactions on the basis of the redox states of the TPQ cofactor (Scheme 1). In the reductive half-reaction initiating from the oxidized cofactor (TPQ_{ox}), the amine substrate reacts with the C5 carbonyl oxygen of TPQ_{ox} to form the first intermediate, the substrate Schiff base. The catalytic base, assigned to an invariant aspartic acid residue, then abstracts the C1 proton of substrate, forming the product Schiff base intermediate ($TPQ_{pim}H^+$) with reduction of the cofactor ring. Hydrolysis of $TPQ_{pim}H^+$ yields the product aldehyde and the reduced cofactor in the aminoresorcinol form (TPQ_{amr}). This part of the reaction is believed to proceed independently of the copper ion.[10] The oxidative half-reaction consists of the steps from TPQ_{amr} to TPQ_{ox} and involves the net two-proton and two-electron transfers from TPQ_{amr} to dioxygen, during which the copper ion has been thought to play an essential role by serving as an electron mediator between TPQ_{amr} and O_2. This role of copper was first proposed on the basis of the observation for the temperature-dependent, rapid equilibrium between the Cu^{2+}/TPQ_{amr} state and the Cu^{1+}/topa semiquinone (TPQ_{sq}) state, suggesting the latter is kinetically competent.[11,12] However, recent kinetic studies on the oxidative half-reaction have been interpreted in terms of initial one-electron reduction of O_2 occurring directly from the Cu^{2+}/TPQ_{amr} couple but not from the Cu^{1+}/TPQ_{sq} couple. Here, the copper ion remains in the divalent state and provides electrostatic stabilization of the superoxide anion intermediate, rather than being reduced to Cu^{1+}.[13−15]

The catalytic role of the tightly bound copper in CAO from a variety of sources has been probed by substitution with other divalent metal cations.[10,14,16−20] In those studies, the Cu^{2+} was removed first by reduction to Cu^{1+} by addition of either dithionite or an amine substrate under anaerobic conditions followed by extensive dialysis against KCN and EDTA. However, the removal of copper was often incomplete, and the resultant "Cu-depleted" (Cu_{dep}) enzymes were significantly active due to the remaining copper, which thereby made it difficult to quantitatively interpret the activities observed for the enzymes subsequently reconstituted with other divalent metal ions (such as Ni^{2+} and Co^{2+}). In a study of yeast CAO, the residual activities were abolished by incubation with an inhibitor phenylhydrazine, prior to reconstitution of the enzyme with Co^{2+}.[14]

In this study, we have nearly completely removed the copper ion from the recombinant phenylethylamine oxidase from *Arthrobacter globiformis* (AGAO). The Cu_{dep}-enzyme containing less than 1/2500 mol atom of copper per mol of enzyme subunit, and showing only negligible activity, was reconstituted with various divalent metal ions. Spectroscopic properties and kinetics of the fully metal-substituted enzymes are reported here, together with the crystal structures of the Co^{2+}- and Ni^{2+}-substituted enzymes.

Experimental Section

Materials. Anhydrous $CoCl_2$ (99.999%), anhydrous $ZnCl_2$ (99.999%), and $NiCl_2 \cdot 6H_2O$ (99.9999%) were purchased from Aldrich Chemicals. All buffers were prepared using water with resistance greater than 16.7 MΩ cm, obtained from a NANOpureII system (Barnstead) and further passed over a Chelex column (Bio-Rad). All glass and plastic wares were thoroughly acid-washed and then rinsed with the Chelex-treated

(5) Janes, S. M.; Mu, D.; Wemmer, D.; Smith, A. J.; Kaur, S.; Maltby, D.; Burlingame, A. L.; Klinman, J. P. *Science* **1990**, *248*, 981−987.
(6) Matsuzaki, R.; Fukui, T.; Sato, H.; Ozaki, Y.; Tanizawa, K. *FEBS Lett.* **1994**, *351*, 360−364.
(7) Cai, D.; Klinman, J. P. *Biochemistry* **1994**, *33*, 7647−7653.
(8) Cai, D.; Klinman, J. P. *J. Biol. Chem.* **1994**, *269*, 32039−32042.
(9) Choi, Y. H.; Matsuzaki, R.; Fukui, T.; Shimizu, E.; Yorifuji, T.; Sato, H.; Ozaki, Y.; Tanizawa, K. *J. Biol. Chem.* **1995**, *270*, 4712−4720.
(10) Rinaldi, A.; Gialtosio, A.; Floris, G.; Medda, R.; Finazzi-Agro, A. *Biochem. Biophys. Res. Commun.* **1984**, *120*, 242−249.
(11) Dooley, D. M.; McGuirl, M. A.; Brown, D. E.; Turowski, P. N.; McIntire, W. S.; Knowles, P. F. *Nature* **1991**, *349*, 262−264.
(12) Turowski, P. N.; McGuirl, M. A.; Dooley, D. M. *J. Biol. Chem.* **1993**, *268*, 17680−17682.
(13) Su, Q.; Klinman, J. P. *Biochemistry* **1998**, *37*, 12513−12525.
(14) Mills, S. A.; Klinman, J. P. *J. Am. Chem. Soc.* **2000**, *122*, 9897−9904.
(15) Schwartz, B.; Olgin, A. K.; Klinman, J. P. *Biochemistry* **2001**, *40*, 2954−2963.
(16) Suzuki, S.; Sakurai, T.; Nakahara, A.; Manabe, T.; Okuyama, T. *Biochemistry* **1983**, *22*, 1630−1635.
(17) Collison, D.; Knowles, P. F.; Mabbs, F. E.; Rius, F. X.; Singh, I.; Dooley, D. M.; Cote, C. E.; McGuirl, M. *Biochem. J.* **1989**, *264*, 663−669.
(18) Agostinelli, E.; Morpurgo, L.; Wang, C.; Giartosio, A.; Mondovi, B. *Eur. J. Biochem.* **1994**, *222*, 727−732.
(19) Agostinelli, E.; De Matteis, G.; Mondovi, B.; Morpurgo, L. *Biochem. J.* **1998**, *330*, 383−387.
(20) Padiglia, A.; Medda, R.; Pedersen, J. Z.; Finazzi-Agro, A.; Lorrai, A.; Murgia, B.; Floris, G. *J. Biol. Inorg. Chem.* **1999**, *4*, 608−613.

water before use. The synthesis and spectroscopic characterization of model compounds for TPQ_{ox}, TPQ_{imq},[21] and TPQ_{amr} were described previously.[22,23] A model compound for TPQ_{pim}[24] was generated in situ by the reaction of the TPQ_{amr} model compound[22] and *n*-propylaldehyde as previously described.[23]

Disruption of Catalase Genes in *E. coli* Host Cells. In our previous studies,[6,25,26] the recombinant AGAO was purified from the overproducing *Escherichia coli* cells transformed with the enzyme gene. However, care had to be taken to separate AGAO from a catalase derived from the host *E. coli* cells. This catalase has a very intense absorption at 400 nm, which coincides with that of TPQ_{ox}. Thus, to minimize the catalase contamination, two (*katG* and *katE*) of the three catalase genes contained in the chromosome of the host *E. coli* BL21 (DE3) strain were disrupted by the P1 phage-mediated transduction and homologous recombination. Briefly, the *katE* gene was first disrupted using the phage lysate obtained from a catalase-deficient *E. coli* mutant UM120 (*thi-1 HfrH katE12::Tn10*),[27] and the *katG* gene was then disrupted from the chromosome of the *katE*-deleted *E. coli* BL21 (DE3) using the phage lysate obtained from another catalase-deficient *E. coli* mutant SN0027 (*supE44 hsdR endA1 pro thi katG::Tn5*).[28] The resultant *katGE*-disrupted *E. coli* BL21 (DE3) cells (designated CD03) produced AGAO as efficiently as the original strain upon transformation with the expression plasmid pEPO-02 carrying the enzyme gene[6] and showed only a very low activity of catalase in the cell extracts, which was probably derived from the third catalase gene (*katP*). The *katP* gene was not disrupted, because it appeared to be minimally required for the aerobic growth of *E. coli*, quenching peroxide species produced within the cells.

Enzyme Purification and Assay. The enzyme was overproduced in *E. coli* CD03/pEPO-02 cells grown in the copper-limited medium and purified in the inactive, precursor form (designated apo-AGAO) to >99% homogeneity on SDS-PAGE and without detectable catalase activity.[6] The purified apo-AGAO was converted to the active form containing copper and TPQ (holo-AGAO) by incubation with 0.5 mM $CuSO_4$ at 30 °C for 30 min in 50 mM HEPES buffer, pH 6.8, or by dialysis against 50 mM HEPES buffer containing 50 μM $CuSO_4$ at 4 °C for 12 h. The enzyme activity was assayed by the peroxidase-coupled method as described previously.[6] The assay for O_2 consumption was performed with a standard Clark-type oxygen electrode (Toko Chemical Laboratories). To the water-jacketed sample chamber, 30 °C, was added the enzyme (0.11 μM subunit) in 50 mM HEPES buffer, pH 6.8 (final volume, 1.0 mL). Before the reaction was started by addition of substrate (20 μM 2-phenylethylamine), the incubations were allowed to equilibrate for at least 20 min until reaching a constant level of O_2 concentration, which was maintained by bubbling with an N_2/O_2-mixed gas through a gas mixer (Mini-Gascom PMG-1, Kofloc). Steady-state kinetic parameters were determined on the basis of the ping-pong bi-bi mechanism, by changing the concentration of either substrate (2-phenylethylamine or O_2) while keeping a saturating concentration of the other substrate, and calculated by fitting the data to nonlinear regression curves of the Michaelis−Menten equation using Kaleidagraph version 3.0 (Abelbeck Software). Protein concentrations were determined from extinction coefficients at 280 nm of 12.3 and 13.2 for 1% (w/v) solutions of apo- and holo-AGAO, respectively.[6]

Determination of TPQ_{ox} and Metal Contents. For determination of the TPQ_{ox} content in the holo-AGAO, the enzyme (5 μM subunit, in 0.5 mL of 50 mM HEPES buffer, pH 6.8) was titrated with a freshly prepared solution of 0.1 mM phenylhydrazine, added in 2 μL aliquots. The sample was incubated at 30 °C until no further increase in absorbance at 432 nm was observed, indicating that the formation of the phenylhydrazine adduct of TPQ_{ox} was completed (~3 min for all of Cu-, Co-, and Ni-AGAO), and the absorbance values were plotted against molar amounts of the phenylhydrazine added.[6] Metal contents were analyzed with a Shimadzu AA-6400G atomic absorption spectrophotometer equipped with a GFA-6500 graphite furnace atomizer using commercially available metal standard solutions.

Preparation of Metal-Substituted AGAO. Cu_{dep}-AGAO was prepared according to the method described by Suzuki et al.[16] with some modifications for keeping anaerobic conditions more strictly: a 300 μL solution of holo-AGAO (~100 mg/mL) was dialyzed at 4 °C for 2−3 h against 500 mL of 50 mM HEPES buffer, pH 6.8, containing 50 mM sodium dithionite. Before each dialysis, metal-free HEPES and potassium phosphate buffers used were purged for a minimum of 1 h with pyrogallol-scrubbed Ar gas.[29] Solid KCN was then added to the buffer to a final concentration of 10 mM, and dialysis was continued overnight in a glovebag filled with O_2-free Ar gas. The remaining cyanide was removed anaerobically by extensive dialysis against 1 L of metal-free 50 mM HEPES buffer, pH 6.8, containing 1 mM EDTA, and then the EDTA was removed by dialysis against 1 L of metal-free 50 mM HEPES buffer, pH 6.8. The Cu_{dep}-AGAO obtained was found to contain less than 0.004 mol atom of copper per mol of enzyme subunit by metal analysis and possess only 0.06% of the original activity when assayed without addition of copper ions (see Results). Reconstitution of Cu_{dep}-AGAO with various divalent metal ions was accomplished by adding a metal solution (final concentration, 0.5 mM) to 0.1 mM Cu_{dep}-AGAO in 50 mM HEPES buffer, pH 6.8 (total volume, 1 mL), and incubating at 30 °C for at least 3 h. The metal-substituted AGAO thus obtained was dialyzed against 1 L of metal-free 50 mM HEPES buffer, pH 6.8, containing 1 mM EDTA and finally against 1 L of metal-free 100 mM potassium phosphate buffer, pH 7.3.

Spectrophotometric Measurements. Rates of anaerobic reduction of the metal-substituted enzyme with excess amine substrate were measured at 5 °C with either a Unisoku RSP-601-03 (for Co- and Ni-AGAO) or an Applied Photophysics SX.17MV (for Cu-AGAO) rapid-scan stopped-flow spectrophotometer with a mixing cell volume of 40 and 20 μL, respectively. Typically, equal volumes (about 30 μL each) of the solutions of enzyme (0.15−0.27 mM subunit) and substrate (3.4 mM 2-phenylethylamine), which had been thoroughly deaerated using a vacuum line and repressurized with N_2 gas, were mixed, and the spectra were recorded at every 1 ms in a wavelength region of 350−800 nm (for Co- and Ni-AGAO) or at every 2.56 ms in a wavelength region of 250−800 nm (for Cu-AGAO). Oxidative half-reactions of the substrate-reduced, metal-substituted enzymes with dioxygen were measured at 30 °C with a Hewlett-Packard 8452A photodiode-array spectrophotometer. The enzyme (final concentration, 60 μM subunit) was first reduced with a substoichiometric amount of substrate (48 μM 2-phenylethylamine) to prevent the catalytic turnover upon addition of dioxygen. The enzyme and substrate solutions were kept in a vacuum-type glovebox (Iuchi, SGV-65V) filled with 99.999% Ar gas for at least 2 h before mixing in a screw-capped quartz cuvette. To prevent contamination of O_2 in the glovebox, an O_2-scrubbing column (Chromatography Research Supplies, Inc., Model-1000 Oxygen

(21) The model compound for TPQ_{imq} (zwitterionic, net neutral) was originally prepared as a model compound for the substrate Schiff base (adducts formed between TPQ_{ox} and cyclohexylamine or *N*-methylbenzylamine). In solution, the corresponding iminoquinone form of TPQ_{ox} exists only as a deprotonated anion where the net charge is fully delocalized to give a λ_{max} at ~450 nm. The spectrum of the zwitterionic substrate Schiff base model compound has a λ_{max} at 350 nm that shifts to ~450 nm upon deprotonation to give a spectrum essentially identical to that of the deprotonated, delocalized iminoquinone. The substitution of an alkyl group onto the imine nitrogen seems not to affect the spectroscopic properties of the iminoquinone. For details, see ref 22.

(22) Mure, M.; Klinman, J. P. *J. Am. Chem. Soc.* **1995**, *117*, 8707−8718.
(23) Mure, M.; Klinman, J. P. *Methods Enzymol.* **1995**, *258*, 39−52.
(24) The model compound for the neutral product Schiff base was prepared with *n*-propylaldehyde instead of phenylacetoaldehyde. Because the aromatic ring of the phenylacetoaldehyde is not conjugated to the reduced TPQ ring, the spectroscopic properties of TPQ_{pim} prepared with propylaldehyde or phenylacetoaldehyde will be identical.
(25) Matsuzaki, R.; Suzuki, S.; Yamaguchi, K.; Fukui, T.; Tanizawa, K. *Biochemistry* **1995**, *34*, 4524−4350.
(26) Matsuzaki, R.; Tanizawa, K. *Biochemistry* **1998**, *37*, 13947−13957.
(27) Nakagawa, S.; Ishino, S.; Teshiba, S. *Biosci. Biotechnol. Biochem.* **1996**, *60*, 415−420.
(28) Loewen, P. C.; Triggs, B. L. *J. Bacteriol.* **1984**, *160*, 668−675.
(29) Mure, M.; Klinman, J. P. *J. Am. Chem. Soc.* **1993**, *115*, 7117−7127.

Trap, with an indicator) was set in the line between the Ar gas cylinder and the glovebox. The amount of trace O_2 was monitored by the change in the UV/vis absorbance spectrum of 10% (w/v) pyrogallol in 0.1 N HCl upon mixing with 2 M KOH in the glovebox, and none was detected. The O_2-saturated HEPES buffer (120 μL) (50 mM, pH 6.8; $[O_2] \approx 1$ mM) was then introduced to the substrate-reduced enzyme solution (30 μL) through a silicon rubber septum using a gastight syringe. The first-order rate constants for the absorption changes were obtained by least-squares exponential fits of the absorbance at fixed wavelengths using Igor Pro version 3.1 (Wave Metrics, Inc.) or Kaleidagraph.

Resonance Raman Spectroscopy. Resonance Raman scattering was excited at 514.5 nm with an Ar^+ ion laser (Spectra Physics, 2017) and detected with a CCD detector (Princeton Instruments) attached to a triple polychromator (JASCO, NR-1800). The excitation laser beam power was adjusted to 70 mW at the sample point. Measurements were carried out at ambient temperature with the enzyme solution (about 50 μL) placed in a spinning cell (3000 rpm). The data accumulation time was 200 s. Raman shifts were calibrated with acetone and toluene, and the resolution of the Raman bands was ± 1 cm^{-1}.

Crystallization. Cu-, Co-, and Ni-AGAO were crystallized at 16 °C by the microdialysis method. The protein concentration in the dialysis button (volume, 50 μL) was 10 mg/mL, and the reservoir solution contained 1.05 M potassium sodium tartrate as a precipitant in 25 mM HEPES buffer, pH 6.8.[30] For all enzymes, platelet-like crystals with approximate dimensions of $0.2 \times 0.4 \times 0.1$ mm appeared within 2 weeks. After further growth of the crystals was allowed, the buttons were transferred into the new reservoir solution containing 45% (v/v) glycerol added as a cryoprotectant. The crystals were mounted on thin nylon loops (ϕ, 0.2−0.3 mm) and frozen by flash cooling to 100 K in a cold N_2 gas stream.

Data Collection and Processing. Diffraction data sets were collected at 100 K with the synchrotron X-radiation ($\lambda = 1.00$ Å), using an ADSC CCD detector (for Co-AGAO) or the Sakabe Weissenberg camera (for Ni-AGAO) in the beam-line station 6A or 18B, respectively, at the KEK Photon Factory (Tsukuba, Japan), or with the synchrotron X-radiation ($\lambda = 0.700$ Å), using a MAR CCD detector (for Cu-AGAO) in the station BL44B2 at the SPring-8 (Hyogo, Japan). The data were processed and scaled using MOSFLM[31] and SCALA[32] for Co- and Cu-AGAO, or DENZO/SCALEPACK[33] for Ni-AGAO. These crystals were found to belong to the space group *C*2 with unit cell dimensions that were different from those of the wild-type Cu-AGAO crystals analyzed at an ambient temperature.[30] The asymmetric unit comprised two monomers derived from different dimer molecules with the cell volume twice that of Cu-AGAO solved previously. The two-fold crystallographic axis deviated slightly from the *b* axis, giving rise to a strong supperlattice effect[30] and breaking down the symmetry. Therefore, to compare the large *C*2 cells of the crystals analyzed at 100 K with the small *C*2 cell of Cu-AGAO analyzed at an ambient temperature, we adopted *I*2 cells, a different cell choice of the space group *C*2, where only the length of the *c* axis was doubled, by transforming the index values of the observed diffraction data. As a result, the asymmetric unit was composed of two subunits derived from the same dimer molecule. The details and statistics of data collection are summarized in Table 1.

Structure Determination and Refinements. An initial model for the AGAO dimer was generated by 180° rotation around the crystallographic two-fold axis of the monomer coordinates (PDB accession code 1AVK) without solvent molecules. The program used for refinements and calculation of the electron-density maps was X-PLOR version 3.1.[34] Manual rebuilding and assignment of solvent molecules were performed using QUANTA version 97 (Accelrys, San Diego, CA). After rigid-body refinement, initial structures of Co-, Ni-, and Cu-AGAO were further refined through simulated annealing at 3000 K and several cycles of positional and *B*-factor refinements. Metal ions were assigned on the basis of the highest peaks in the respective $2F_o - F_c$ maps; water molecules and residues in the active site region were carefully modeled using the $2F_o - F_c$, $F_o - F_c$, and omit maps. The details and statistics of crystallographic refinement for Cu-, Co-, and Ni-AGAO structures are also given in Table 1. The coordinates for Co-, Ni-, and Cu-AGAO have been deposited in the Protein Data Bank with the accession codes 1IQX, 1IQY, and 1IU7, respectively.

Table 1. Statistics of Data Collection and Refinement

	Cu-AGAO	Co-AGAO	Ni-AGAO
Data Collection			
original cell			
Space group	*C*2	*C*2	*C*2
unit cell dimensions: *a*, *b*, *c* (Å)	192.96, 62.63, 157.52	192.94, 62.77, 157.99	192.90, 62.84, 157.80
β (deg)	117.68	117.62	117.62
transformed cell			
space group	I2	I2	I2
unit cell dimensions: *a*, *b*, *c* (Å)	157.79, 62.63, 183.96	157.99, 62.77, 184.19	157.80, 62.84, 184.07
β (deg)	111.74	111.85	111.80
number of observations	1 290 645	480 123	364 483
number of unique reflections	172 839	155 223	146 419
$d_{max} - d_{min}$ (Å)	25.2 − 1.7	10 − 1.8	10 − 1.8
overall completeness (%)	94.0	99.8	94.8
overall R_{merge} (%)[a]	4.0	7.4	3.8
Refinement Statistics			
$d_{max} - d_{min}$ (Å)	7 − 1.8	10 − 2.0	10 − 1.8
residues in the core ϕ, φ regions (%)	88.6	88.3	87.7
number of non-hydrogen atoms	10 980	10 693	10 646
number of solvent atoms	1242	955	908
average temperature factors			
main-chain (Å^2)	17.5	16.6	20.5
side-chain atoms (Å^2)	19.2	17.9	21.6
solvent atoms (Å^2)	31.7	25.7	29.6
RMS deviation from ideal values			
bond lengths (Å)	0.010	0.010	0.010
bond angles (deg)	1.8	1.8	1.8
refinement features	bulk solvent correction	bulk solvent correction	bulk solvent correction
residual *R* (%)[b]	20.9	21.1	20.8
free residual *R* (%)[c]	25.2	26.0	26.0

[a] $R_{merge} = \sum h \sum i |I_{h,i} - \langle I_h \rangle| / \sum h \sum i I_{h,i}$, where $I_{h,i}$ is the intensity value of the *i*th measurement of *h*, and $\langle I_h \rangle$ is the corresponding mean value of I_h for all *i* measurements. [b] $R = \sum ||F_o| - |F_c|| / \sum |F_o|$. [c] Free residual *R* is an *R* factor of the X-PLOR refinement evaluated for 5% of the reflections that were excluded from the refinement.

Results

Depletion of Cu^{2+} from Holo-AGAO. The Cu_{dep}-enzyme obtained in this study contained only 0.004 mol atom of Cu^{2+} per mol of subunit (Table 2), which was significantly lower

(30) Wilce, M. C.; Dooley, D. M.; Freeman, H. C.; Guss, J. M.; Matsunami, H.; McIntire, W. S.; Ruggiero, C. E.; Tanizawa, K.; Yamaguchi, H. *Biochemistry* **1997**, *36*, 16116−16133.
(31) Leslie, A. G. W. *Joint CCP4 EESF-EACMB Newsletter on Protein Crystallography*; SERC Daresbury Laboratory: Warrington, U.K., 1992.
(32) Collaborative Computational Project Number 4. *Acta Crystallogr.* **1994**, *D50*, 760−763.
(33) Otwinowski, Z.; Minor, W. *Methods Enzymol.* **1997**, *276*, 307−326.
(34) Brunger, A. T.; Adams, P. D.; Clore, G. M.; DeLano, W. L.; Gros, P.; Grosse-Kunstleve, R. W.; Jiang, J. S.; Kuszewski, J.; Nilges, M.; Pannu, N. S.; Read, R. J.; Rice, L. M.; Simonson, T.; Warren, G. L. *Acta Crystallogr.* **1998**, *D54*, 905−921.

Table 2. Characteristics of Cu_{dep}- and Metal-Substituted AGAO

enzyme	specific activity (U/mg)	TPQ_{ox}/subunit	metal content (mol atom/subunit)[b]	K_m (μM) 2-PEA[c]	K_m (μM) O_2	k_{cat} (s^{-1})[d] 2-PEA[c]	k_{cat} (s^{-1})[d] O_2
Cu-AGAO	67.5 (100)[a]	0.68 ± 0.01	0.880 ± 0.002 (Cu)	2.5 ± 0.0	20.8 ± 6.0	75.7 ± 0.8	110 ± 7
Cu_{dep}-AGAO	0.04 (0.06)	ND[e]	0.0041 ± 0.0002 (Cu)				
Cu_{rec}-AGAO	57.9 (86)	0.58 ± 0.01	0.97 ± 0.04 (Cu)				
Co-AGAO	1.51 (2.2)	0.67 ± 0.02	0.0063 ± 0.0004 (Cu) 1.060 ± 0.001 (Co)	1.9 ± 0.1	16.3 ± 5.8	1.51 ± 0.01	1.24 ± 0.07
Ni-AGAO	0.58 (0.9)	0.78 ± 0.02	0.0088 ± 0.0002 (Cu) 0.800 ± 0.024 (Ni)	3.8 ± 0.2	18.3 ± 2.4	1.30 ± 0.02	1.13 ± 0.04
Zn-AGAO	0.04 (0.06)	ND[e]	0.0084 ± 0.0004 (Cu) 1.390 ± 0.004 (Zn)				

[a] Relative activities. [b] Values for the metals indicated in parentheses. [c] 2-Phenylethylamine. [d] Calculated from V_{max} values determined with 2-phenylethylamine or O_2 as varied substrate. [e] Not detected.

Scheme 2. Reduction of Cu^{2+}/TPQ_{ox} to Cu^{+}/TPQ_{red} with Sodium Dithionite

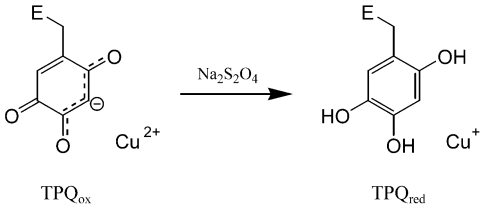

than the remaining Cu^{2+} contents (2−30% of the initial contents) obtained in previous studies.[10,14,16−20] The remaining catalytic activity of Cu_{dep}-AGAO was also less than 0.1% of that of the original Cu-enzyme, when assayed without adding Cu^{2+}.[35] The near complete removal of Cu^{2+} was achieved by first reducing Cu^{2+}/TPQ_{ox} to the Cu^{+}/trihydroxybenzene form of reduced TPQ (TPQ_{red}; see Scheme 2) under strictly anaerobic conditions, followed by addition of KCN to dissociate Cu^{+} from the active site. KCN was added after the reduction as it also reacts with TPQ_{ox}, possibly forming a cyanohydrin-like adduct.[36,37] O_2 must be rigorously excluded because reoxidation of Cu^{+}/TPQ_{red} will greatly reduce the efficiency of removal of the very tightly bound Cu^{2+}. Nearly 90% of the original enzyme activities were recovered by reconstitution with Cu^{2+} (Table 2), showing that the enzyme protein had not been irreversibly denatured during the procedure.

Reconstitution with Divalent Metal Ions. Following the dithionite treatment and Cu^{2+} removal from holo-AGAO, TPQ_{ox} was reduced to TPQ_{red} (Scheme 2), as shown by the loss of the 480 nm absorption band diagnostic of TPQ_{ox} (Figure 1a). In marked contrast to the reduced form of a TPQ model compound,[14,29] the enzyme-linked TPQ_{red} in Cu_{dep}-AGAO was resistant to reoxidation by air, staying in the reduced form for a long period (several days) when kept in 50 mM HEPES buffer, pH 6.8. It was air-oxidized gradually in a weak alkaline buffer (50 mM Bicine, pH 9.0) with a pseudo-first-order rate constant (k_{obs}) of 4.2×10^{-3} min^{-1} at 30 °C, estimated from the reappearance of the 480 nm absorption band of TPQ_{ox}. When the Cu_{dep}-protein was unfolded in 8 M urea, rapid oxidation to TPQ_{ox} was observed (k_{obs} = 0.23 min^{-1} at 30 °C, pH 6.8), showing that the TPQ_{red} exposed to the solvent is readily oxidized. Very rapid oxidation of TPQ_{red} linked in the native

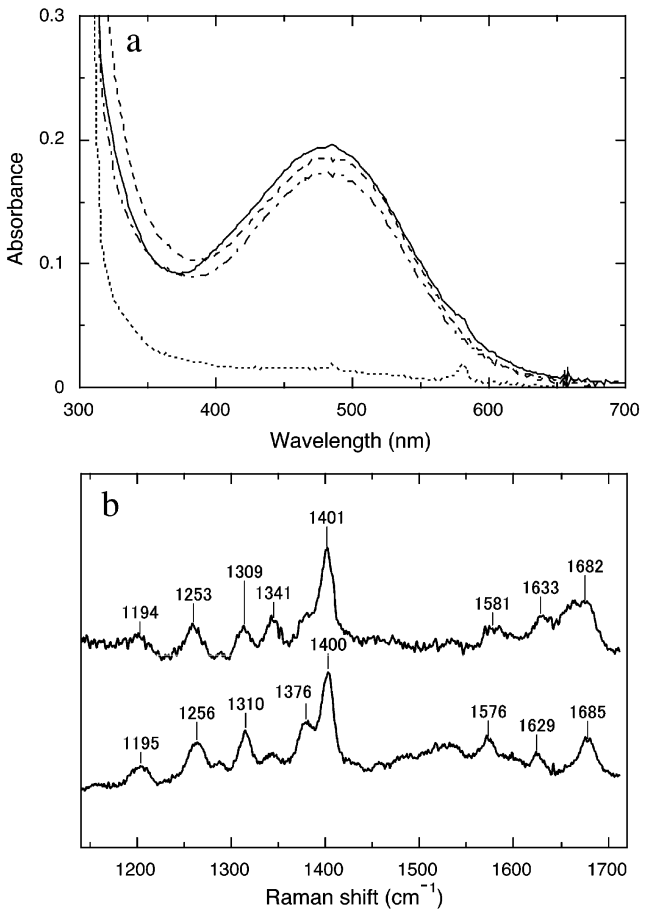

Figure 1. UV/vis absorption and resonance Raman spectra of wild-type and metal-substituted AGAO. (a) Absorption spectra of Cu_{dep}-AGAO with the cofactor in the TPQ_{red} state (·····), and the fully oxidized forms of Cu-AGAO (−), Co-AGAO (− - −), and Ni-AGAO (- - - -) were measured in 50 mM HEPES buffer, pH 6.8, at subunit concentrations of 0.15 mM. (b) Resonance Raman spectra of the oxidized Cu-AGAO (upper) and Co-AGAO (lower) were measured at room temperature in the same buffer as in (a). The ordinate scales are normalized with the intensity of the 1400 cm^{-1} band of Co-AGAO, and the spectra are offset for clarity. Frequency shifts calibrated with acetone and toluene standards (not shown) are indicated above the peaks. See the Experimental Section for instrumental conditions.

apoprotein was observed upon reconstitution of the Cu_{dep}-enzyme with several divalent metal ions, among which the original metal ion, Cu^{2+}, was most effective, regenerating TPQ_{ox} within a few minutes (k_{obs} = 1.0 min^{-1} at 30 °C, pH 6.8). Besides the Cu^{2+}, Co^{2+} and Ni^{2+} were also found effective, although with lower rates (Co^{2+}, k_{obs} = 0.57 min^{-1}; Ni^{2+}, k_{obs} = 0.065 min^{-1}; at 30 °C, pH 6.8), leading to the fully oxidized

(35) The very low activity observed with the Cu_{dep}-enzyme can be accounted for by the trace amount of remaining Cu^{2+} (Table 2), suggesting that the fully copper-depleted form of enzyme is completely inactive.
(36) McGuirl, M. A.; Brown, D. E.; Dooley, D. M. *J. Biol. Inorg. Chem.* **1997**, *2*, 336−342.
(37) He, Z.; Zou, Y.; Greenaway, F. T. *Arch. Biochem. Biophys.* **1995**, *319*, 185−195.

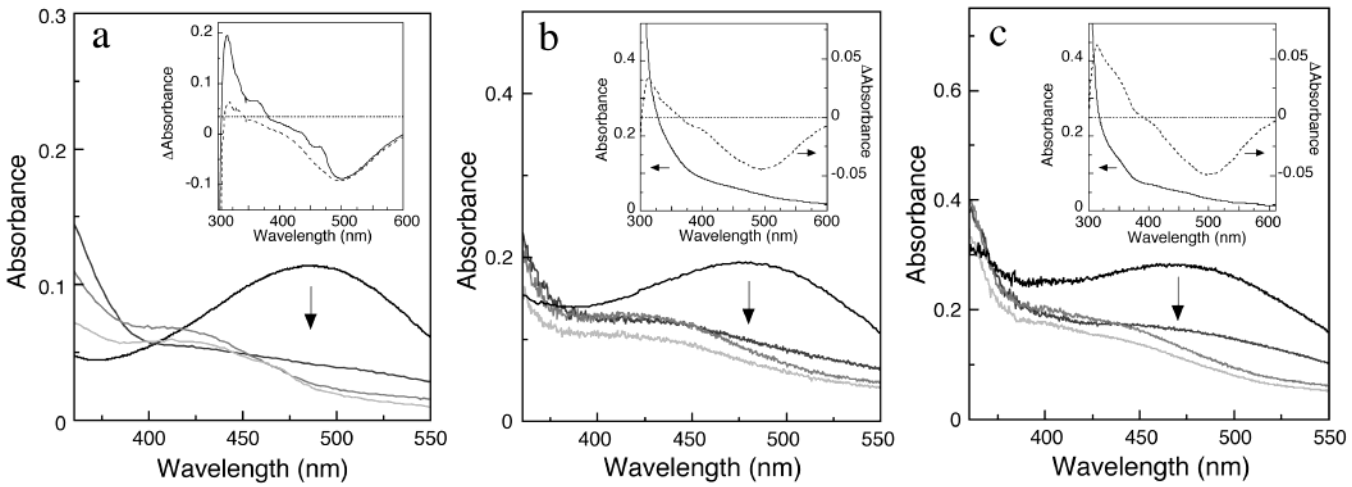

Figure 2. Rapid-scan stopped-flow spectral measurements of the anaerobic reaction of the metal-substituted AGAO with excess substrate. Cu-AGAO (0.15 mM subunit) (a), Co-AGAO (0.27 mM subunit) (b), and Ni-AGAO (0.27 mM subunit) (c) were mixed anaerobically at 5 °C with 3.4 mM 2-phenylethylamine. The spectra are at 0, 1.28, 6.4, and 21.8 ms (Cu-AGAO), and at 0, 1.5, 5.5, and 31 ms (Co- and Ni-AGAO) after mixing (darker spectra represent earlier times). The 0 time spectrum (before mixing) has been corrected for enzyme concentration. Inset: (a) Spectra of the substrate-reduced Cu-AGAO at 21.8 ms (·····) and 1.3 s (−) after mixing, both subtracted by the 0 ms spectrum (TPQ_{ox} form). (b, c) Equilibrium absorption spectra of Co- (b), and Ni-AGAO (c), measured in 50 mM HEPES buffer, pH 6.8, at 30 °C after anaerobic incubation of Co- and Ni-AGAO (50 μM subunit) with excess 2-phenylethylamine (0.5 mM) for 1 h (−). Difference spectra of the reduced form minus the oxidized form are also shown (·····).

TPQ after incubation for a sufficiently long time (>1 h) (Figure 1a). However, other divalent metal ions such as Zn^{2+}, Ca^{2+}, Mg^{2+}, and Mn^{2+} did not support O_2-based oxidation of the enzyme-linked TPQ_{red} even after incubation for 24 h. We have shown that Zn^{2+} does bind to Cu_{dep}-AGAO by atomic absorption spectrometry (Table 2).[38]

Characterization of Metal-Substituted AGAO. Catalytic properties as well as the amounts of TPQ_{ox} and metal ions in the initial Cu-, Cu_{dep}-, Cu-reconstituted (Cu_{rec}), Co-, and Ni-AGAO are summarized in Table 2. Metal contents determined by atomic absorption spectrometry revealed nearly stoichiometric incorporation of each metal ion, as well as the absence of adventitiously bound Cu^{2+}. Although the catalytic activities of Co- and Ni-AGAO were considerably lower than those of the initial Cu- and Cu_{rec}-enzymes, they were significantly more active than Cu_{dep}-AGAO. The amounts of TPQ_{ox} in the Co- and Ni-substituted enzymes, as determined by titration with phenylhydrazine, were comparable with those of the initial Cu- and Cu_{rec}-enzymes. Also, the reactivities of TPQ_{ox} in Co- and Ni-AGAO toward the inhibitor were similar to that in Cu-AGAO where the hydrazone formation was completed within about 3 min. Furthermore, UV/vis absorption and resonance Raman spectra were essentially the same as those of the Cu-enzyme (Figure 1a,b), indicating that the electronic state of TPQ_{ox} within the enzyme active site is not affected very much by the nature of the bound metal ions. Also shown in Table 2 are steady-state kinetic parameters of the native Cu- and metal-substituted enzymes. K_m values for both substrates (2-phenylethylamine and O_2) of Co- and Ni-AGAO were similar to those of the native Cu-enzyme. In contrast, k_{cat} values of the metal-substituted enzymes, determined with a saturated concentration of either substrate (2-phenylethylamine or O_2), were considerably lower, suggesting that the bound metal ion participates in the catalytic process, rather than in substrate binding.

Reductive Half-Reaction of Co- and Ni-AGAO. To elucidate the cause of the low activities of the metal-substituted enzymes, the reductive half-reaction was analyzed by rapid-scanning stopped-flow spectrophotometry. Upon anaerobic mixing of Co- or Ni-AGAO with excess 2-phenylethylamine at 5 °C, the 480 nm absorption band derived from TPQ_{ox} disappeared within 2−6 ms after mixing (Figure 2b,c), with estimated rate constants of about 700 and 300 s^{-1} for Co- and Ni-AGAO, respectively. Thus, the spectral changes associated with the reduction of TPQ_{ox} in both Co- and Ni-AGAO by amine substrate are rapid, as observed for the native Cu-enzyme, in which the 480 nm absorption of TPQ_{ox} disappears within 1.5 ms after mixing (k_{obs} > 1000 s^{-1}) (Figure 2a). These results are consistent with the generally accepted mechanism for the reductive half-reaction, where the bound metal ion does not play a direct role in catalysis.[10] In the substrate-reduced Cu-AGAO, TPQ_{sq}, exhibiting typical absorption bands at about 365, 440, and 470 nm, is detected (appears about 30 ms after mixing) due to the equilibrium between the Cu^{2+}/TPQ_{amr} state and the Cu^{1+}/TPQ_{sq} (Figure 2a, inset),[25,41] as in the case of other CAOs.[11,12] On the other hand, TPQ_{sq} was not detected in the substrate-reduced Co- and Ni-AGAO, and TPQ exists mostly as TPQ_{amr} (Figure 2b,c, insets).[42] Presumably, the $1e^-$-transfer from TPQ_{amr} to the bound metal ion does not occur in the substrate-reduced, metal-substituted enzymes because of the energetically unfavorable monovalent states of those metal ions (Co^+, Ni^+). Furthermore, the TPQ_{amr} observed in the UV/vis difference spectra of the substrate-reduced Co- and Ni-AGAO contained an extra absorption at around 350 nm (Figure 2b,c, insets). This is in contrast to the TPQ_{amr} observed in the substrate-reduced, wild-type (Cu^{2+}) CAOs from bovine serum[13] and yeast[43] and also a model compound (Figure 5a), which

(38) Our recent crystallographic analysis of apo-AGAO soaked with Zn^{2+} ion has shown that Zn^{2+} occupies the Cu^{2+}-binding site (Kim, M., unpublished results), as reported for HPAO.[39,40]
(39) Cai, D.; Williams, N. K.; Klinman, J. P. *J. Biol. Chem.* **1997**, *272*, 19277−19281.
(40) Chen, Z.; Schwartz, B.; Williams, N. K.; Li, R.; Klinman, J. P.; Mathews, F. S. *Biochemistry* **2000**, *39*, 9709−9717.
(41) Hirota, S.; Iwamoto, T.; Kishishita, S.; Okajima, T.; Yamauchi, O.; Tanizawa, K. *Biochemistry* **2001**, *40*, 15789−15796.
(42) TPQ_{amr} formed in the substrate-reduced Co- and Ni-AGAO is assigned to a neutral form on the basis of the λ_{max} values (~310 nm) observed in the difference spectra (Figure 2, insets).[13,23,59]
(43) Plastino, J.; Green, E. L.; Snders-Loehr, J.; Klinman, J. P. *Biochemistry* **1999**, *38*, 8204−8216.

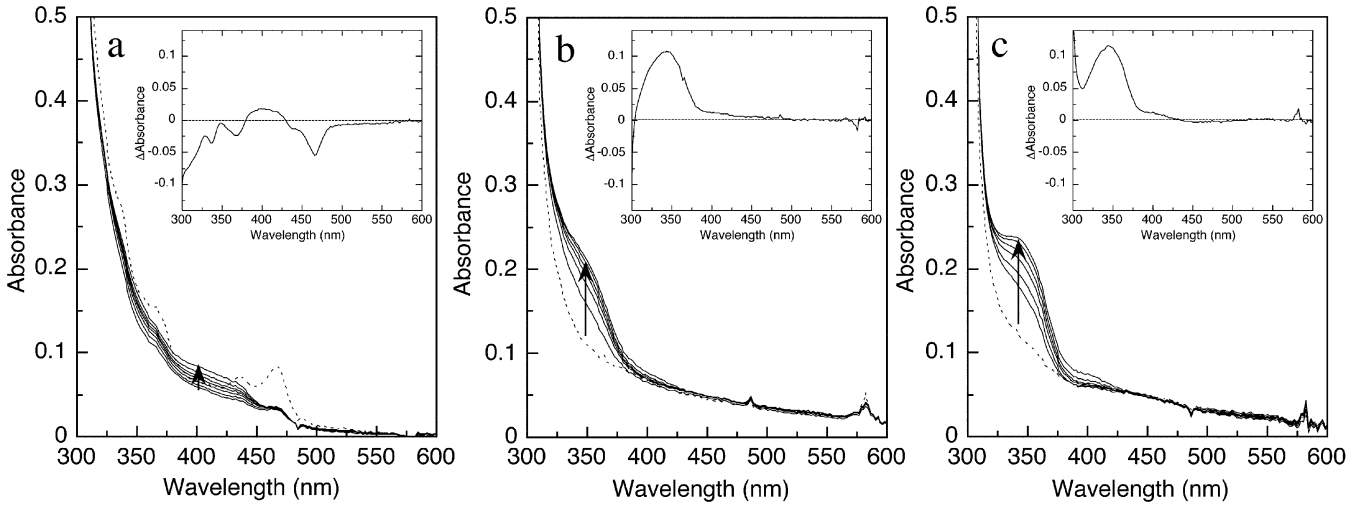

Figure 3. Slow formation of the product Schiff base in the substrate-reduced AGAO. Cu- (a), Co- (b), and Ni-AGAO (c) (60 μM subunit for each enzyme) were reduced anaerobically with 48 μM 2-phenylethylamine in 50 mM HEPES buffer, pH 6.8, at 30 °C in the glovebox. After about 5 min, 1.2 mM 2-phenylacetaldehyde was added. Absorption spectra shown are those measured at 230, 330, 530, 730, 1130, and 1930 s for Cu-AGAO (a), at 203, 403, 603, 803, 1203, and 2203 s for Co-AGAO (b), and at 238, 438, 638, 838, 1238, and 2238 s for Ni-AGAO (c), after addition of 2-phenylacetaldehyde. The spectra shown with dotted lines are those measured without addition of 2-phenylacetaldehyde for $t = 0$ of the product addition. Arrows indicate the direction of the spectral change. The first-order rate constants for the formation of the product Schiff base in Co- and Ni-AGAO were calculated by least-squares exponential fitting of the absorbance changes at 346 nm as 0.0031 and 0.0023 s^{-1}, respectively. Inset: Difference spectra, where the $t = 0$ spectrum was subtracted from the final spectrum of each form of the enzyme.

exhibit only an absorbance maximum at around 305−310 nm and no extra features. Subsequently, it was found that this 350 nm species gradually built in following the reductive half-reaction in the absence of dioxygen (no further spectral change was observed after 6 min). This suggested that there was a back reaction between TPQ_{amr} and the product aldehyde. To support this assignment, we measured spectral changes of the substrate-reduced enzymes in the presence of excess product, 2-phenylacetaldehyde (Figure 3). Clearly, there were gradual increases of absorbance at around 350 nm, showing that TPQ_{amr} produced in the reductive half-reaction did react with the product aldehyde, presumably forming the neutral product Schiff base. Using TPQ_{amr} and TPQ_{pim} model compounds (Figure 5a), we estimated the amount of the product Schiff base at $t = 0$ s as approximately 10−15% in Co-AGAO and 20−25% in Ni-AGAO (Figure 5b). In contrast, no such accumulation of the species was observed in Cu-AGAO when incubating with excess product aldehyde under anaerobic conditions (Figure 3a). Although a slow loss of TPQ_{sq} was detected, no distinct spectral features were observed to build in.

Oxidative Half-Reaction of Co- and Ni-AGAO. As the reductive half-reaction proceeded at a much faster rate than k_{cat} in all forms of AGAO, the origin of the differences in the catalytic activities of the native and metal-substituted enzymes was then pursued in the oxidative half-reaction. We have recently shown that the substrate-reduced Cu-AGAO reacts very rapidly with O_2 even at 5 °C, faster than the mixing dead time of the stopped-flow measurement ($t_{1/2} < 1$ ms; $k_{obs} > 1000$ s^{-1}), as indicated in the rapid loss of TPQ_{sq}. The later generation of TPQ_{ox} is the rate-limiting step of the oxidative half-reaction of AGAO under single turnover conditions.[41] The oxidative half-reaction of Cu-AGAO is complete within 1 s. However, the oxidative half-reaction of Co- and Ni-AGAO proceeded rather slowly when compared to Cu-AGAO, so that the process could be monitored with a conventional spectrophotometer by manually adding the O_2-saturated buffer to the substrate-reduced enzyme (Figure 4a,c). The spectral changes occurring during the oxidative half-reaction of Co- and Ni-AGAO are shown in the difference spectra (Figure 4b,d). Initially, there was a clear absorbance maximum characteristic of the neutral TPQ_{amr} at around 310 nm in the spectra of both Co- and Ni-AGAO. The absorbance characteristic of TPQ_{amr} decayed within the first 10−20 s after mixing. After about 20 s, a prominent feature appeared at around 350−360 nm that tailed into the 310 nm absorbance. After about 80 s, the broad absorbance peak with a λ_{max} at around 350−360 nm disappeared concomitantly with the appearance of the broad absorption maximum at 480 nm with an isosbestic point (around 400 nm). This indicates that TPQ_{ox} is formed from the intermediate absorbing at about 360 nm. By comparison with the spectra of TPQ model compounds (Figure 5a), the 360 nm peak can be assigned to an iminoquinone form (TPQ_{imq}) of the oxidized cofactor (zwitterionic, net neutral). Spectral simulations using TPQ model compounds (Figure 5a) provided difference spectra (Figure 5c) closely resembling those of the oxidative half-reaction of Co- and Ni-AGAO. One difference between the model system and the enzyme systems is the presence of a broader absorbance associated with TPQ_{imq} in the latter as compared to that in the former.

The absorbance changes at 306 and 360 nm show an initial fast phase over the first 20 s. We could not fit these changes accurately due to the interfering absorbance of TPQ_{pim}, and we were only able to obtain estimates for k_{obs} for the fast decay at 306 nm (0.18 s^{-1} for Co-AGAO and 0.17 s^{-1} for Ni-AGAO). The time-dependence of the absorption changes at selected wavelengths (306, 360, and 480 nm) after 80 s was analyzed and fitted to single-component pseudo-first-order kinetics by the least-squares method (Figure 6). Rate constants show that the initial reaction of TPQ_{amr} with dioxygen is significantly slower in Co- and Ni-AGAO than it is in the wild-type Cu-enzyme.[41] The fast phase for the decay at 306 nm for both Co- and Ni-AGAO most likely represents the reaction of TPQ_{amr}

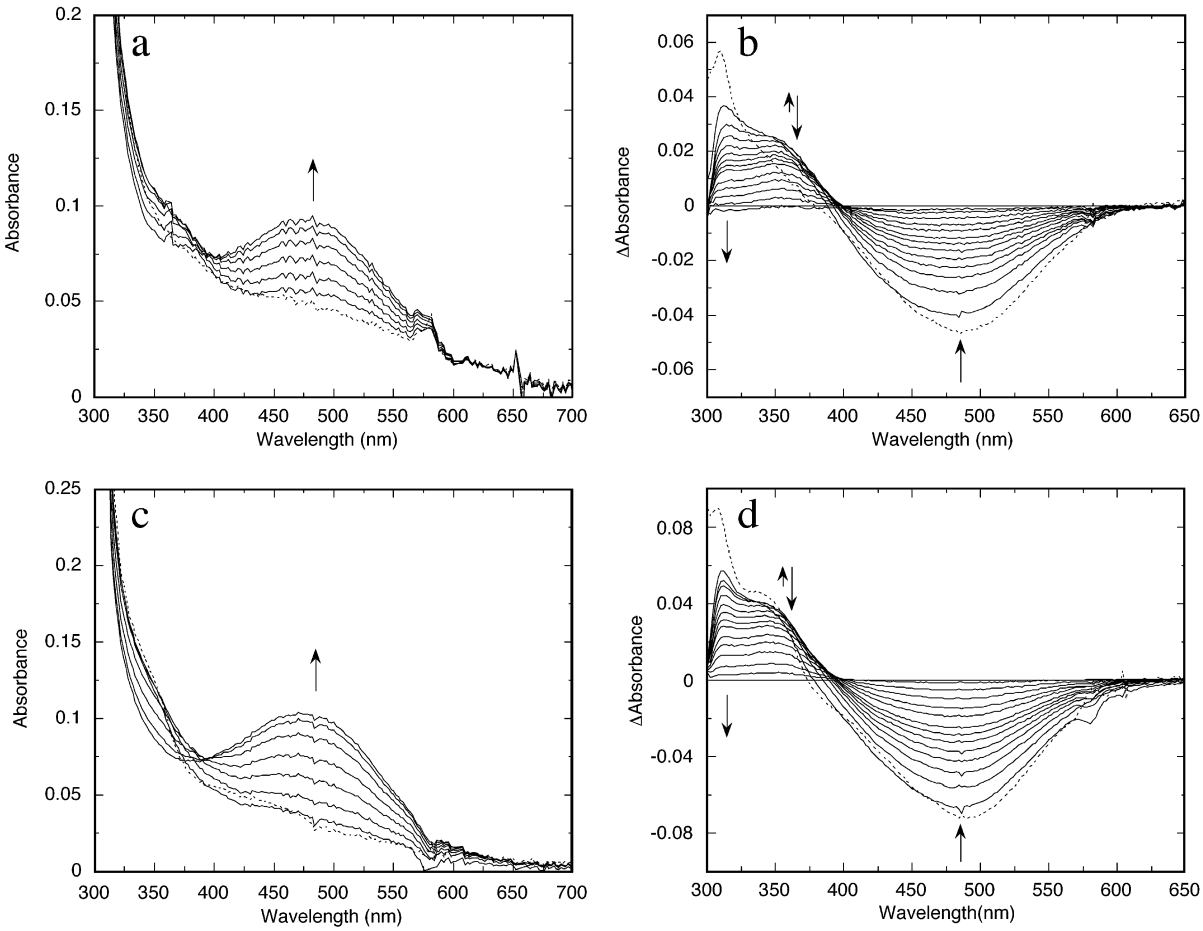

Figure 4. Spectral changes during the oxidative half-reaction of Co- and Ni-AGAO. Absorption spectra of Co-AGAO (a) (at 9, 19, 39, 69, 119, and 199 s) and Ni-AGAO (c) (at 12, 22, 42, 72, 122, 202, and 402 s) shown are those measured after addition of 120 μL of the O_2-saturated buffer (50 mM HEPES, pH 6.8) at 30 °C (final concentration of the enzymes, 60 μM subunit). Prior to the oxidative half-reaction, both enzymes were reduced anaerobically with 48 μM 2-phenylethylamine in an Ar gas-filled glovebox. Difference spectra of the oxidative half-reaction were obtained by subtracting the spectrum of each oxidized enzyme (at 1800 s after the mixing) from those at 9, 19, 29, 39, 49, 59, 69, 79, 99, 119, 149, 199, and 299 s for Co-AGAO (b) and those at 12, 22, 32, 42, 52, 62, 72, 82, 102, 122, 152, 202, and 302 s for Ni-AGAO (d). Dotted lines indicate absorption (a, c) and difference spectra (b, d) for the same concentrations of substrate-reduced Co- and Ni-AGAO diluted by the O_2-free buffer under anaerobic conditions, showing the spectra at $t = 0$ s. Arrows indicate the direction of the spectral change.

and dioxygen. The value we obtained for the rate of loss of TPQ_{amr} for Ni-AGAO is comparable to the rate reported for the formation of TPQ_{imq} in Ni-AGAO under stopped-flow conditions (0.17 s^{-1}), although the latter experiment was performed at 5 °C.[41] The slow phase of the decay of absorbance at 306 nm is associated with the loss of absorbance at 350−360 nm and probably represents the consumption of TPQ_{imq}. TPQ_{imq} should be the immediate precursor to TPQ_{ox}, and as expected the slow phase of 306 nm decay occurs at the same rate as the appearance of TPQ_{ox} at 480 nm. The low catalytic activities of the metal-substituted enzymes can be explained by the marked decrease in the efficiency of oxidative half-reaction.

Crystal Structures of Cu-, Co-, and Ni-AGAO Solved at 100 K. To identify structural differences between the native and metal-substituted enzymes, we have determined the crystal structures of Cu-, Co-, and Ni-AGAO at 100 K (Table 1). In the Cu-AGAO structure previously solved at an ambient temperature,[30] the electron density for the TPQ cofactor was insufficient to define the orientation of the quinone group; two orientations differing by a rotation of 180° about the $C^{\beta}-C^{\gamma}$ bond were equally probable. Therefore, the structure of Cu-AGAO has also been determined in this study at 100 K to compare the three AGAO structures solved under the same conditions. After refinement, the structure of Cu-AGAO determined at a low temperature was proven to be practically identical to the previous structure (PDB code, 1AV4), except for the electron density that unambiguously defined the single orientation of the TPQ cofactor (see below).

As expected, both the Co^{2+} and the Ni^{2+} in the metal-substituted enzymes were found to occupy the Cu^{2+} site in the Cu-AGAO structure. Also, the overall polypeptide fold and the positions of most of the side chains were almost identical to those of Cu-AGAO. Comparison of each of the Co- and Ni-AGAO structures with the Cu-AGAO structure gave root-mean-square deviations of 0.44 and 0.40 Å, respectively, for the coordinates of all main-chain atoms. Significant differences were noted only for the residues located in the active site, including crystallographically identified water molecules. For a detailed description of the structural differences (see below), the $2F_o - F_c$ electron density map and the hydrogen-bonding network around the active site of Co-AGAO are represented in Figure 7, the structure of Ni-AGAO being essentially the same. Several important residues, the bound metal ions, and water molecules in the active site of the three structures (Cu-, Co-, and Ni-AGAO) are also superimposed for comparison (Figure 8a).

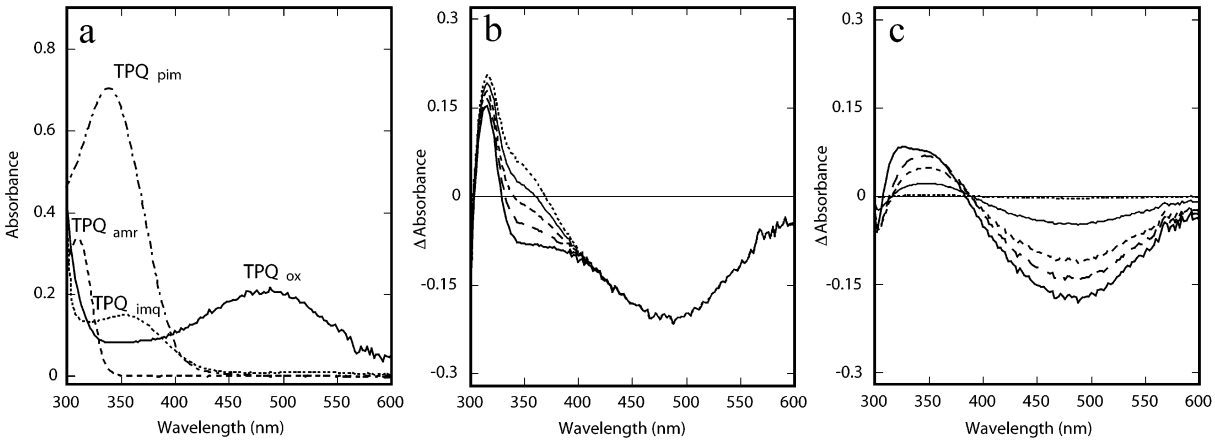

Figure 5. (a) Spectra of TPQ model compounds. TPQ_{amr}, an aminoresorcinol form of TPQ_{red}; TPQ_{imq}, an iminoquinone form of TPQ (neutral form); TPQ_{ox}, an oxidized form of TPQ; TPQ_{pim}, a product Schiff base form of TPQ (neutral form). Concentrations of the model compounds are 0.1 mM. All spectra were taken at 25 °C. TPQ_{amr} and TPQ_{ox} are in 0.02 M potassium phosphate buffer at pH 7.2 ($\mu = 0.2$ with NaCl). TPQ_{imq} and TPQ_{pim} are in anhydrous acetonitrile. The spectrum of TPQ_{amr} has been red-shifted by 14 nm to make the λ_{max} comparable to that seen in Co- and Ni-AGAO (shifted from 296 to 310 nm). (b) Difference spectra at different relative concentrations of TPQ_{amr} and TPQ_{pim}, where TPQ_{ox} has been subtracted from the admixed spectra for comparison with the $t = 0$ s spectra of Co- and Ni-AGAO in the oxidative half-reaction. Dark solid line, 100% TPQ_{amr}; broken line, TPQ_{amr}:TPQ_{pim} = 95:5; dashed line, TPQ_{amr}:TPQ_{pim} = 90:10; light solid line TPQ_{amr}:TPQ_{pim} = 85:15; dotted line, TPQ_{amr}:TPQ_{pim} = 80:20. (c) Difference spectra using TPQ model compounds in the oxidative half-reaction of Co-AGAO where the contribution of each component was estimated from the kinetic plot in Figure 6a. Dark solid line (9 s), TPQ_{amr}:TPQ_{imq}:TPQ_{ox}:TPQ_{pim} = 23:53:14:10; broken line (19 s), ratio = 3:62:30:5; dashed line (29 s), ratio = 1:51.5:45:2.5; light solid line (79 s), ratio = 0:23:76:1; dotted line (199 s), ratio = 0:2:98:0.

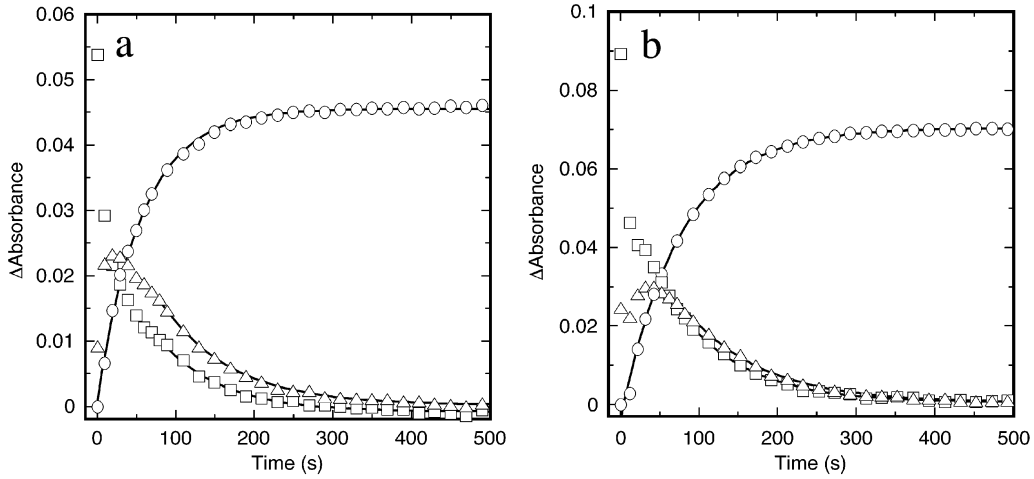

Figure 6. Time course of absorbance changes during the oxidative half-reaction of Co- (a) and Ni-AGAO (b) traced at fixed wavelengths. Spectral changes shown in Figure 4a,c were plotted at 306 (□), 360 (△), and 480 (○) nm. The plots in the slow phase (for 306 and 360 nm, after 80 s) were fitted to pseudo-first-order kinetics by the least-squares method using $y = [\Delta A]_{max} \cdot \exp(-k_{obs}t)$ or $[\Delta A]_{max}\{1 - \exp(-k_{obs}t)\}$, where $[\Delta A]_{max}$ is equivalent to the absorption difference at $t = 0$ (at 306 and 360 nm) or $t =$ infinity (at 480 nm) (solid curves). Estimated k_{obs} values at 306 (decrease), 360 (decrease), and 480 nm (increase) were 0.027, 0.011, and 0.018 s^{-1}, respectively, for Co-AGAO, and 0.0094, 0.0098, and 0.013 s^{-1}, respectively, for Ni-AGAO.

The most pronounced difference is found in the conformation of one of the three metal-binding His residues, His592 (Figure 8a). In Co- and Ni-AGAO, the imidazole side chain of His592 adopts a conformation different from that in Cu-AGAO, rotating counterclockwise (viewed against main-chain atoms) by ∼60° about the $C^{\alpha}-C^{\beta}$ bond. Furthermore, while the Cu^{2+} ion in the Cu-AGAO structure is five-coordinate [three imidazole nitrogen atoms of His431, His433, and His592 plus two water molecules, one (Wat1) at an equatorial position and the other (Wat2) at an axial position of the distorted square-pyramidal geometry[30] (Figure 8d)], both metal ions in the Co- and Ni-AGAO structures have an additional water ligand (Wat3) that is absent in Cu-AGAO. Thus, the Co^{2+} and Ni^{2+} ions are six-coordinate and exhibit octahedral geometry (Figure 8b,c). Bond angles and lengths involved in these metal coordination structures are summarized in Table 3. The metal-to-Wat2 distances in Co- and Ni-AGAO are shorter by 0.4 Å than in Cu-AGAO and are close to those of the other metal−ligand bond lengths in each structure. The long Cu^{2+}-to-Wat2 distance is typical for Cu^{2+} (d^9) as it is in a Jahn−Teller system, giving rise to the distorted square-pyramidal geometry. Co^{2+} (d^7) also takes a Jahn−Teller system but is known to show much smaller distortions from regular geometry than Cu^{2+}.[45]

Besides the metal ligands, the side chain of Met602 in Co- and Ni-AGAO is tilted by ∼150° about the $C^{\alpha}-C^{\beta}$ bond, with the *S*-methyl group positioned differently in each of the three forms (Figure 8a). Furthermore, the side chain of Tyr296, located near the end of the substrate channel and assumed to be a "gate" to the active site,[30] appears to have a "gate-open" conformation in all of the present AGAO structures, as modeled on the basis of the unambiguous electron density for this residue (Figure 7a), which was missing in the previous AGAO

(44) Esnouf, R. M. *J. Mol. Graphics* **1997**, *15*, 132−134.
(45) Rulisek, L.; Havlas, Z. J. *Chem. Phys.* **2000**, *112*, 149−157.

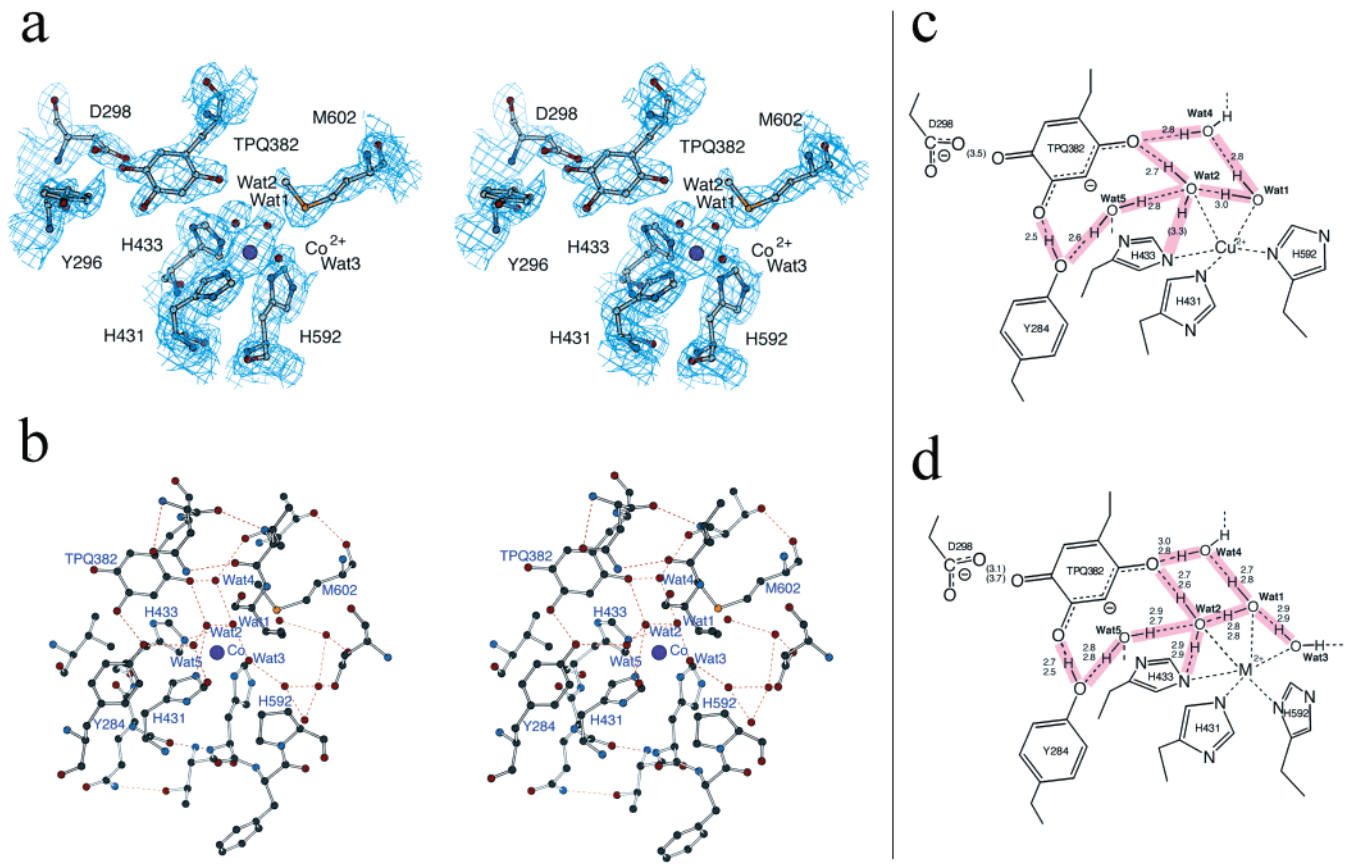

Figure 7. Active site structure of Co-AGAO. (a) Stereo diagram of the $2F_o$-F_c electron density map around the active site of Co-AGAO, contoured at a 1.5-σ level. Residues and water molecules conserved in the active site are shown in a ball-and-stick model. (b) Stereo diagram of the active site of Co-AGAO with hydrogen bonds shown in red dotted lines. The figures were drawn using BOBSCRIPT.[44] (c,d) Schematic drawing of the hydrogen-bonding network (shaded in pink) around the active site of Cu-AGAO (c) and metal-substituted AGAO (d). Lengths (Å) of hydrogen bonds (atom-atom distances of O···O and O···N) are indicated [in (d): first row, Co-AGAO; second row, Ni-AGAO]. Distances between close but non-hydrogen-bonding atoms are also shown in parentheses.

structures.[30] The carboxyl group of the presumed catalytic base, Asp298, functioning in the proton abstraction from the substrate Schiff base, has also different rotation angles about the $C^{\beta}-C^{\gamma}$ bond in the three structures (Figure 8a). However, except for the difference in the metal coordination structures, subtle conformational differences of these residues are likely within the flexibility allowed for them and are presumably not derived from the metal substitution.

In contrast to the previous Cu-AGAO structure solved at an ambient temperature,[30] the electron densities for TPQ_{ox} of Co-, Ni-, and Cu-AGAO structures solved at 100 K clearly defined a single orientation of the quinone group with the C2═O atom closest to the metal ion and the C5═O atom in proximity to the catalytic base Asp298 (Figure 7a). This orientation of the TPQ ring is identical with those in the active form structures of a CAO from *E. coli* (ECAO)[46−48] and *Hansenula polymorpha* (HPAO)[49] and appears to be held by hydrogen bonds formed between the TPQ C2═O atom and Wat2 (2.7 Å in Co-AGAO, 2.6 Å in Ni-AGAO, and 2.7 Å in Cu-AGAO) and between the TPQ C4−O atom and the hydroxyl group of Tyr284 (2.7 Å in Co-AGAO, 2.5 Å in Ni-AGAO, and 2.5 Å in Cu-AGAO) (Figure 7d), which is an invariant residue in all CAOs. There are also conserved water molecules (Wat4 and Wat5), which do not participate as a metal ligand but are involved in the hydrogen-bonding network around the active site (Figures 7b, 8a). The patterns of hydrogen bonds involving these metal-coordinating and non-coordinating water molecules (Figure 7c,d) are essentially the same as those in the Cu-AGAO structure, despite the considerable difference in the metal coordination structures described above.

Discussion

The present studies with AGAO, in which Cu^{2+} was replaced by Co^{2+} or Ni^{2+}, have shown that the spectral properties of TPQ_{ox} (Figure 1), the reactivity to phenylhydrazine, and K_m values for amine substrate and dioxygen (Table 2) are little affected by the nature of the bound metal ion. Anaerobic reduction of TPQ_{ox} with excess 2-phenylethylamine in Co- and Ni-AGAO is also rapid, as in Cu-AGAO (Figure 2). The distance between the C5 carbonyl oxygen of TPQ_{ox} and the

(46) Parsons, M. R.; Convery, M. A.; Wilmot, C. M.; Yadav, K. D. S.; Blakeley, V.; Corner, A. S.; Phillips, S. E. V.; McPherson, M. J.; Knowles, P. F. *Structure* **1995**, *3*, 1171−1184.
(47) Wilmot, C. M.; Murray, J. M.; Alton, G.; Parsons, M. R.; Convery, M. A.; Blakeley, V.; Corner, A. S.; Palcic, M. M.; Knowles, P. F.; McPherson, M. J.; Phillips, S. E. V. *Biochemistry* **1997**, *36*, 1608−1620.
(48) Wilmot, C. M.; Hajdu, J.; McPherson, M. J.; Knowles, P. F.; Phillips, S. E. *Science* **1999**, *286*, 1724−1728.
(49) Li, R.; Klinman, J. P.; Mathews, F. S. *Structure* **1998**, *6*, 293−307.

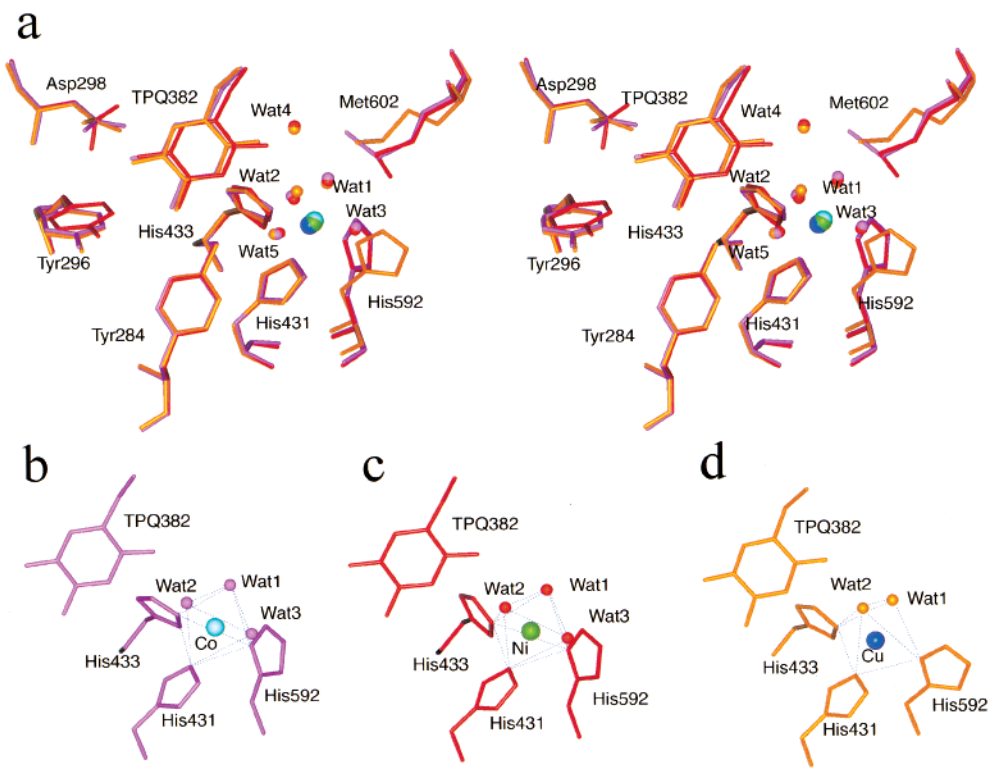

Figure 8. Stick models of the active site residues of AGAO. (a) Stereo diagram of the superimposed active sites of Cu-, Co-, and Ni-AGAO, shown in orange, magenta, and red, respectively. Metal-coordinating and noncoordinating water molecules are also shown in the same color codes. Cu^{2+}, Co^{2+}, and Ni^{2+} are represented by purple, sky blue, and green spheres, respectively. (b, c, d) Metal-coordination structures of Co-, Ni-, and Cu-AGAO, respectively. Dotted lines in blue are drawn for easier understanding of the coordination structures. The figures were drawn by Insight II (MSI, San Diego, CA).

Table 3. Bond Distances and Angles in Metal Coordination Structures of Cu-, Co-, and Ni-AGAO

	Cu-AGAO			Co-AGAO			Ni-AGAO		
		angle (deg)			angle (deg)			angle (deg)	
	distance from Cu (Å)	X–Cu–His431 $N^{\epsilon 2}$	X–Cu–Wat1	distance from Co (Å)	X–Co–His431 $N^{\epsilon 2}$	X–Co–Wat1	distance from Ni (Å)	X–Ni–His431 $N^{\epsilon 2}$	X–Ni–Wat1
His431 $N^{\epsilon 2}$	2.1		162	2.2		163	2.0		168
His433 $N^{\epsilon 2}$	2.2	98	85	2.3	92	85	2.3	88	90
His592 $N^{\delta 1}$	2.2	95	90	2.3	106	90	2.4	104	88
Wat1	2.0			2.0			2.0		
Wat2	2.7	84	78	2.3	82	81	2.3	84	84
Wat3				2.2	92	89	2.1	92	89

catalytic base (Asp298) is similarly short in the structures of Cu-, Co-, and Ni-AGAO (Figure 5c,d), supporting the efficient proton abstraction from the substrate C1 position, possibly by proton tunneling.[50] It has been established that TPQ_{ox} has a certain degree of mobility in the active site.[30,43,46,51,52] For the reductive half-reaction to occur, the mobility of TPQ must be regulated such that the C5═O atom must be facing toward the substrate binding site. This regulation is achieved by hydrogen-bonding interactions between TPQ_{ox} and a number of key active-site residues and metal- and nonmetal-coordinated water molecules. Any disruption of these interactions, such as site-directed mutations, causes a loss of activity. Clearly, the structural similarity between the Co-, Ni-, and Cu-AGAO active sites shows that TPQ_{ox} is held in the correct conformation in all three cases, and this explains how the efficiency of the reductive half-reaction is retained after metal substitution by Co^{2+} and Ni^{2+}.

Altogether, it is evident that the metal ion does not participate directly in the steps of the reductive half-reaction of the catalytic cycle, involving (i) formation of the substrate Schiff base, (ii) abstraction of the substrate C1 proton and protonation of the TPQ C4 (or C2) oxygen atom, forming the product Schiff base, and (iii) hydrolysis of the protonated product Schiff base ($TPQ_{pim}H^+$) releasing the product aldehyde and TPQ_{amr} (Scheme 1). Rather, the metal ion plays a key role in the oxidative half-reaction, as manifested by the slow regeneration of TPQ_{ox} in the reaction with O_2 of the substrate-reduced Co- and Ni-AGAO (Figure 4).

Reaction between TPQ_{amr} and the Product Aldehyde. Following the reduction of TPQ_{ox} by amine substrate, the final product should be the neutral form of TPQ_{amr}, which shows a single absorbance at around 300−310 nm as seen both in BSAO[13] and in an active site base mutant of HPAO.[43] In

(50) Kohen, A.; Klinman, J. P. *Acc. Chem. Res.* **1998**, *31*, 397−404.
(51) Murray, J. M.; Saysell, C. G.; Wilmot, C. M.; Tambyrajah, W. S.; Jaeger, J.; Knowles, P. F.; Phillips, S. E.; McPherson, M. J. *Biochemistry* **1999**, *38*, 8217−8227.
(52) Murray, J. M.; Kurtis, C. R.; Tambyrajah, W.; Saysell, C. G.; Wilmot, C. M.; Parsons, M. R.; Phillips, S. E.; Knowles, P. F.; McPherson, M. J. *Biochemistry* **2001**, *40*, 12808−12818.

Scheme 3. Hydrolysis of $TPQ_{pim}H^+$ to TPQ_{amr} and Back Reaction between TPQ_{amr} and Product Aldehyde, Yielding Neutral TPQ_{pim}

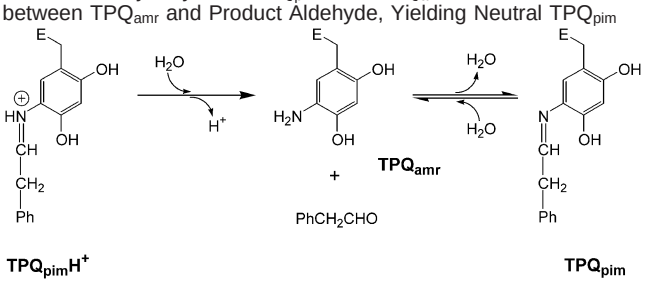

Cu-AGAO, we saw the formation of TPQ_{sq} following the reduction of TPQ_{ox} as seen in other forms of CAOs.[41] In Co- and Ni-AGAO, in addition to TPQ_{amr} absorbing at around 310 nm, an extra spectral feature indicating a chromophore with a λ_{max} at around 350 nm built in 5 min after the reduction was complete. Initially, we believed that this species might be TPQ_{imq}; if so, this could be a result of O_2 contamination in the system. However, we were able to achieve strictly anaerobic conditions (see Experimental Section), and yet we were still unable to obtain a clean UV/vis spectrum of TPQ_{amr}. Further, this 350 nm species did not decay to form TPQ_{ox} as would be expected for TPQ_{imq} to TPQ_{ox} (see Oxidative Half-Reaction section). Addition of excess product aldehyde to TPQ_{amr} increased the amount of 350 nm species (Figure 3b,c), enabling its assignment to TPQ_{pim}.

The X-ray crystal structure of the substrate-reduced form of ECAO shows that the product aldehyde can remain bound in the active site.[48] This explains how the product aldehyde could back react with TPQ_{amr} to form TPQ_{pim}, which exists in an equilibrium with TPQ_{amr} (Scheme 3). It has been shown that the protonated form of TPQ_{pim} ($TPQ_{pim}H^+$) undergoes rapid hydrolysis but the neutral form is stable and is not on the reaction pathway.[53] In HPAO, TPQ_{pim} absorbs at 380 nm, but the corresponding model compound absorbs at 340−350 nm (Figure 5a,b). In contrast to Co- and Ni-AGAO, no such back reaction was detected for Cu-AGAO. Although TPQ_{sq} does decay, no 350 nm absorption band accumulated in Cu-AGAO, suggesting that the back reaction is prevented in Cu-AGAO. It is unclear what this loss of TPQ_{sq} represents, but it appears to be an effect of adding excess aldehyde and is not seen after reduction with substoichiometric amounts of substrate. It seems that the hydrolysis of the product aldehyde is more favorable in Cu-AGAO, and this is supported by the relative rates of hydrolysis of TPQ_{imq} to TPQ_{ox} in Cu-, Co-, and Ni-AGAO (see Oxidative Half-Reaction section). The rates of formation of TPQ_{pim} (see Figure 3) are too slow to be on the catalytic pathway. The presence of excess substrate amine during the turnover may help to displace the product aldehyde.

Mechanism of Oxidative Half-Reaction. Shown in Scheme 4 is a possible mechanism for the oxidative half-reaction catalyzed by AGAO, proposed on the basis of this study and previous studies.[13,22,41,43,54] The oxidative half-reaction consists of the net transfer of $2e^-$ and $2H^+$ from TPQ_{amr} to dioxygen, where TPQ_{amr} results from the $2e^-$-reduction of TPQ_{ox} by substrate amine. Following the oxidation of TPQ_{amr}, the products are TPQ_{imq} and hydrogen peroxide. In the absence of O_2, TPQ_{amr}/Cu^{2+} in substrate-reduced Cu-AGAO undergoes rapid disproportionation and exists in equilibrium with TPQ_{sq}/Cu^+,[41,55] similar to what has been observed in other CAOs.[11,56,57] However, under analogous conditions, no TPQ_{sq} was detected in the absorption spectra of the substrate-reduced Co- and Ni-AGAO (Figure 2). As suggested in the previous studies with Co-substituted HPAO[14] and bovine serum amine oxidase (BSAO),[19] the $1e^-$-transfer from TPQ_{amr} to these metal ions is unlikely to occur. It is thus conceivable that the initial step in the oxidative half-reaction of Co- and Ni-AGAO is the direct $1e^-$-reduction of dioxygen by TPQ_{amr} and does not involve any change in the redox state of the metal. However, the initial reaction of TPQ_{amr} with O_2 is much slower in Co- and Ni-AGAO than it is in the native Cu-enzyme.[41] In this way, Cu^{2+} appears to play a key role in the initial step of the oxidative half-reaction. There were only slight differences in K_m values for O_2 of Cu-, Co-, and Ni-AGAO, showing that any putative O_2 binding is unaffected by metal substitution in AGAO (Table 2.)

It is possible that the slow rates of oxidation in Co- and Ni-AGAO versus Cu-AGAO arise from a perturbation of the pK_a of TPQ_{amr}, thereby altering its redox potential. This perturbation has been proposed to originate from different protonation states of the metal-bound water molecules.[14] To undergo facile oxidation, the amino group of TPQ_{amr} must be deprotonated. The pK_a value of TPQ_{amr} is determined as 7.2 in BSAO[13] as compared to 5.9 in the model system.[29] In AGAO, the neutral form of TPQ_{amr} was detected in all three forms of the enzyme (λ_{max} at around 300−310 nm vs no absorption band above 300 nm for protonated TPQ_{amr}),[23] and the initial rates of oxidation are relatively fast. There are no significant structural or electronic differences with respect to TPQ. The crystal structure shows that none of the water ligands on the metal ions are directly hydrogen bonded to TPQ_{ox} and so the metal is unlikely to affect the pK_a of TPQ_{amr}. Further, the relative rates of oxidation of TPQ_{red} (first $pK_a = 9.1$) followed the same trends as those of TPQ_{amr}, that is, $Cu^{2+} \gg Co^{2+} > Ni^{2+}$, where the redox potentials of the neutral forms of TPQ_{amr} and TPQ_{red} are very similar.[29] All of these observations, when taken together, suggest that TPQ_{amr} is in the same protonation state (neutral) in Cu-, Co-, and Ni-AGAO.

In BSAO[13] and HPAO,[14] the rate-limiting step in the oxidative half-reaction has been proposed to be the formation of a cationic TPQ_{sq1} and metal-bound superoxide. If this is correct, the only species that should be detectable in the oxidative half-reaction is TPQ_{amr}. As predicted, we saw no evidence of a semiquinone species in the oxidative half-reaction with Co- and Ni-AGAO. Cationic TPQ_{sq1} has a strong visible absorbance at 430 nm,[58] which is not present in the intermediates we observed. Further, the intermediates did not exhibit absorption spectra resembling that of the TPQ_{sq} species ($\lambda_{max} = 310$, 365, 440, and 470 nm) formed from the disproportionation of TPQ_{amr} and Cu^{2+} in AGAO,[41,55] and other CAOs.[11,56,57] This TPQ_{sq}, shown as TPQ_{sq2} in Scheme 4, has been assigned as either an anionic radical by

(53) Cai, D.; Dove, J.; Nakamura, N.; Sanders-Loehr, J.; Klinman, J. P. *Biochemistry* **1997**, *36*, 11472−11478.
(54) Klinman, J. P. *Chem. Rev.* **1996**, *96*, 2541−2561.
(55) Hirota, S.; Iwamoto, T.; Tanizawa, K.; Adachi, O.; Yamauchi, O. *Biochemistry* **1999**, *38*, 14256−14263.
(56) Warncke, K.; Babcock, G. T.; Dooley, D. M.; McGuirl, M. A.; McCracken, J. *J. Am. Chem. Soc.* **1994**, *116*, 4028−4037.
(57) Steinebach, V.; de Vries, S.; Duine, J. A. *J. Biol. Chem.* **1996**, *271*, 5580−5588.
(58) Bisby, R. H.; Johnson, S. A.; Parker, A. W. *J. Phys. Chem.* **2000**, *B104*, 5832−5839.

Scheme 4. Proposed Mechanism of Oxidative Half-Reaction by Wild-type and Metal-Substituted AGAO

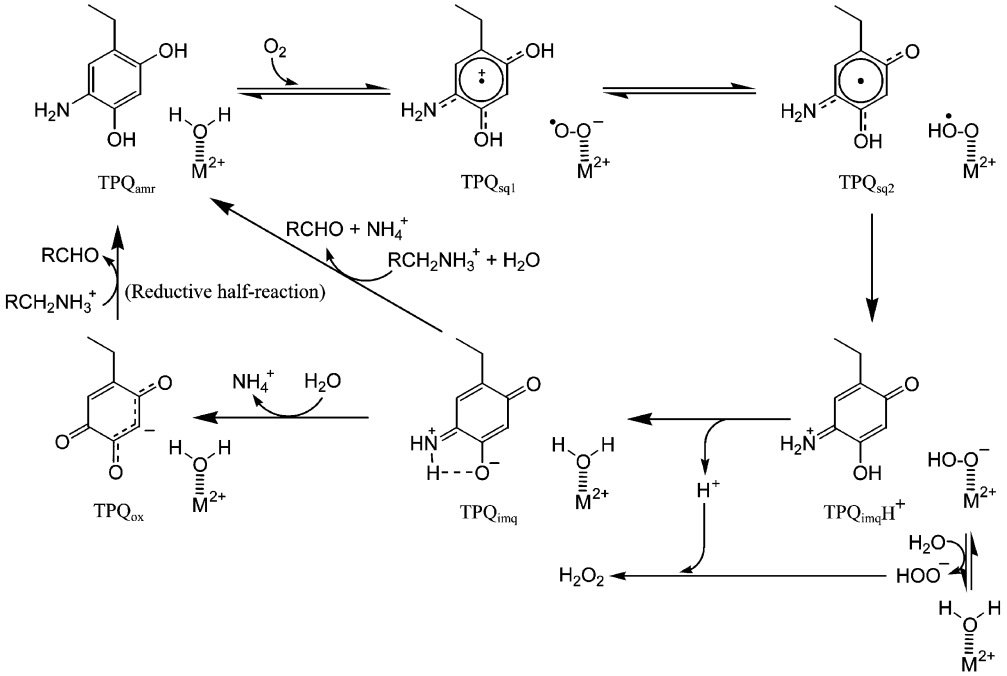

ESEEM[56] or a neutral radical by resonance Raman spectroscopy,[58] where these two species have similar UV/vis absorption spectra.

In contrast to the prediction based on studies of BSAO[13] and HPAO,[14] the intermediate that accumulates in the oxidative half-reaction under single turnover conditions was assigned to be the neutral iminoquinone form of TPQ (TPQ_{imq}), but not the protonated iminoquinone ($TPQ_{imq}H^+$), in comparison to the model study and also in analogy to the substrate Schiff base intermediate observed in BSAO.[59] The 4-hydroxyl group of $TPQ_{imq}H^+$ should be very acidic as in the case of TPQ_{ox} (pK_a = 2.8 in AGAO, unpublished results) and loses the proton readily to solution or possibly to the metal-bound hydroperoxide to assist the release of hydrogen peroxide (Scheme 4).

It was difficult to obtain the precise rate constants for the disappearance of TPQ_{amr} and subsequent formation of TPQ_{imq} in Co- and Ni-AGAO as multiple species absorbed in the same wavelength range. Even so, there is clear evidence that the oxidation of TPQ_{amr} and subsequent formation of TPQ_{imq} occur over about 20 s. This is in clear contrast to Cu-AGAO, where the entire oxidative half-reaction has run its course within 1 s. The k_{obs} for TPQ_{amr} oxidation in Co- and Ni-AGAO estimated from the fast phase probably underestimates the true rate constant, providing a lower limit.[60] The true values would be close to those of k_{cat} for O_2 of both Co- and Ni-AGAO (Table 2), and hence this oxidation may be the rate-limiting step in the catalytic cycle of Co- and Ni-AGAO.

The final step in the oxidative half-reaction under single turnover conditions is the hydrolysis of TPQ_{imq} to regenerate TPQ_{ox}. Under the catalytic turnover conditions, this may not be on the reaction pathway. Here, TPQ_{imq} is thought to react directly with a substrate amine to form the substrate Schiff base (trans-imination reaction). Model studies suggested that the trans-imination is orders of magnitude faster than hydrolysis.[22] The rate of the hydrolysis of TPQ_{imq} to TPQ_{ox} in Co- and Ni-AGAO is surprisingly slow in comparison to that of Cu-AGAO (approximately 1000 times slower).[41] This is consistent with the observation of the presence of a back reaction between the product aldehyde and TPQ_{amr} seen in Co- and Ni-AGAO but being absent in Cu-AGAO. The hydrolysis reactions are somehow perturbed by metal replacement. A possible explanation for this lies in the coordination environment of the metal centers. In oxidized AGAO, Cu^{2+} is five-coordinate, having two water ligands, whereas Co^{2+} and Ni^{2+} are six-coordinate with three water ligands. Crystal structures of ECAO show that Cu^{2+} becomes four-coordinate upon reduction of the enzyme with substrate amine[48] or after an adduct formation with a substrate analogue inhibitor,[47] where one of the water ligands is lost. This remaining water ligand is displaced by a reduced dioxygen species, presumably hydroperoxide (this peroxide species has been observed both crystallographically[48] and spectroscopically[41]), upon oxidation of TPQ_{amr} to form TPQ_{imq}. Cu^{2+} releases water into the active site upon both reduction of TPQ_{ox} and oxidation of TPQ_{amr}. It is possible that neither Co^{2+} nor Ni^{2+} changes their coordination number upon substrate reduction of TPQ_{ox}. This would explain why the back reaction to form TPQ_{pim} occurs readily in Co- and Ni-AGAO but not in Cu-AGAO. In the latter, the released water shifts the equilibrium away from TPQ_{pim} toward aldehyde and TPQ_{amr} (Scheme 3). Further, no peroxide species has been detected in the oxidative half-reaction involving Co- and Ni-AGAO, showing that such an intermediate may be short-lived on the time-scale of TPQ_{ox} formation. When TPQ_{imq} is formed in the metal-replaced systems, there may be fewer free water molecules available for the hydrolysis of TPQ_{imq} to TPQ_{ox} in Co- and Ni-AGAO than

(59) Hartmann, C.; Brzovic, P.; Klinman, J. P. *Biochemistry* **1993**, *32*, 2234−2241.

(60) We measured the oxidative half-reaction of Co- and Ni-AGAO by stopped-flow spectrophotometry, but again we could not obtain an accurate rate constant for the decay of absorbance at 306 nm due to the interfering absorbance of TPQ_{pim}. Therefore, the rate reported for the formation of TPQ_{imq} in Ni-AGAO under stopped-flow conditions (0.17 s^{-1})[41] should also be underestimated.

there is in Cu-AGAO, thus explaining the vast differences in the rates of this reaction between the three systems.

Under the conditions used in this study, we are not able to distinguish whether the two electrons and two protons are transferred from TPQ_{amr} to dioxygen in a consecutive or a concerted fashion. In Scheme 4, we have shown the consecutive mechanism for the sake of clarity.

Role of Cu^{2+}. There have been two roles proposed for how Cu^{2+} may mediate the electron transfer between TPQ_{amr} and dioxygen. One is to form TPQ_{sq} by a disproportionation reaction between Cu^{2+} and TPQ_{amr}.[11,12] The other is to provide a binding site for reduced dioxygen species, thereby driving the reaction.[13−15]

In Co- and Ni-AGAO, the only species seen following the reductive half-reaction are TPQ_{amr} and TPQ_{pim}. There is no evidence for the formation of TPQ_{sq} either directly after the reduction or as a discrete intermediate following the oxidation by dioxygen. This shows that TPQ_{sq} need not form for the oxidative half-reaction to proceed and that no oxidation state change of the metal is required. However, this is not to say that Cu^{1+}/TPQ_{sq} is not on the reaction pathway. Clearly, the initial reaction in the substrate-reduced form of AGAO is much faster when Cu^{2+} is at the active site. The catalytic effect of Cu^{2+} reduction to Cu^{1+} is consistent with this rate acceleration. Our current data can neither confirm nor deny this possibility.[61]

We now address the second proposed role for Cu^{2+}. The oxidation of TPQ_{amr} is associated with the reduction of dioxygen. It is thought that this reduction proceeds in a stepwise manner, where the successive products are superoxide and peroxide. The $1e^-$-reduction of superoxide to peroxide and its protonation to hydroperoxide ($TPQ_{sq2} \rightarrow TPQ_{imq}H^+$, Scheme 4) probably require binding of superoxide to the metal to undergo further $1e^-$-reduction and/or $1H^+$-addition, as proposed in the detailed studies on the oxidative half-reaction of BSAO.[13] Once bound to the metal, superoxide could readily capture an electron and a proton, yielding the hydroperoxide anion ($M^{2+}-{}^-O-OH$, Scheme 4). Binding of a peroxide species to the active site copper has been demonstrated by X-ray crystallography of ECAO[48] and also by the spectrophotometric analysis of the substrate-reduced Cu-AGAO.[41] In the flash-frozen intermediate formed after prolonged aerobic exposure of the ECAO crystals to excess amine substrate (2-phenylethylamine), the dioxygen species was found to occupy the site formerly occupied by the water molecule coordinating axial to the copper in the resting enzyme.[48] In view of the strict conservation of the copper coordination structure in CAOs whose crystal structures have been solved,[30,46−49,62] the binding site for the reduced dioxygen species is probably common to all CAOs, the position being axial to the metal ion (corresponding to Wat2 in AGAO, Figure 8). If the "end-on" binding mode[48] of peroxide to Cu^{2+} with a $Cu^{2+}-O$ distance of 2.8 Å and a $Cu^{2+}-O-O$ angle of 88° holds in AGAO, the bound reduced dioxygen species could form a hydrogen bond to one (Wat5) of the metal-noncoordinating water molecules conserved in the active site (Figure 7b−d). Wat5 is also linked by hydrogen bonds to the TPQ C−O4 atom through the hydroxyl group of the invariant Tyr284 (Figure 7c,d), thus providing an uninterrupted pathway for proton transfer from TPQ_{sq1} to the metal-bound superoxide anion.

In contrast to the metal-bound superoxide ($M^{2+}-OO^{\bullet -}$) or peroxide ($M^{2+}-OO^{2-}$), protonation of a metal-bound hydroperoxide ($M^{2+}-{}^-OOH$) requires prior dissociation from the metal. In ECAO, the hydroperoxide is thought to be bound on the Jahn−Teller axis of Cu^{2+}, as shown by the long metal-to-oxygen bond distance of 2.8 Å.[48] This suggests that hydroperoxide is weakly associated with Cu^{2+}, thereby promoting both binding of reduced oxygen species and release of hydrogen peroxide. In the cases of Co- and Ni-AGAO, the equivalent hydroperoxide binding site, Wat2, would put the metal-to-oxygen bond distance at about 2.3 Å (Table 3), suggesting that the hydroperoxide would be more tightly associated to these metal ions than to Cu^{2+}. Further, the ligand exchange rate of Co^{2+} and Ni^{2+} would be expected to be much slower than that of Cu^{2+}.[63] In this way, the release and subsequent protonation of hydroperoxide would be slower with Co^{2+} and Ni^{2+} than with Cu^{2+}. However, no evidence exists for a hydroperoxide species in the spectra of Co- and Ni-AGAO following the oxidation of TPQ_{amr}. It is possible that the reduced oxygen species are released rapidly in Co- and Ni- as compared to the rate of hydrolysis of TPQ_{imq}. At this point, there are no crystal structures of either the substrate-reduced or the TPQ_{imq} forms of Co- and Ni-AGAO to confirm the presence or absence of bound peroxide. Aside from the metal coordination structure and redox chemistry of Cu^{2+}, there are no other significant differences between the three structures of the oxidized forms that can explain the dramatic difference in reactivity.

The presence of a binding site for reduced oxygen species on the metal in all three forms of AGAO may play a role in controlling the oxidation of TPQ_{red} (trihydroxybenzene form of TPQ) to TPQ_{ox}. Although TPQ_{red} is very stable in the Cu_{dep}-enzyme, when it is fully exposed to solvent, either by denaturation of the protein or as a model compound, it is rapidly oxidized by air to TPQ_{ox} in the absence of a metal ion at a physiological pH. Clearly, in the enzyme active site, there is some barrier to the electron-transfer processes that must be overcome by the presence of these metal ions. In the model system, and presumably in the denatured enzyme, the first e^--transfer between TPQ_{red} and O_2 initiates an autoxidation reaction that may be catalyzed by trace metal ions[64] and which requires freely diffusing radical species, the semiquinone form of TPQ_{red} or superoxide, to propagate the radical chain. In the Cu_{dep}-enzyme, the back electron transfer between the semiquinone and superoxide may occur faster than either the diffusion of superoxide out of the active site or the second e^--transfer which would form TPQ_{ox} and peroxide (analogous to TPQ_{imq} formation, see Scheme 4). The bound Cu^{2+}, Co^{2+}, and Ni^{2+} may be required to both trap the superoxide anion and facilitate the second e^--transfer from the neutral semiquinone form of TPQ_{red} (analogous to TPQ_{sq2}) to the metal-bound superoxide, forming TPQ_{ox} and metal-bound hydroperoxide, in analogy to what has been proposed for the oxidative half-reaction.

(61) A reviewer of this paper suggested that TPQ_{sq} could form in Co^{2+}- and Ni^{2+}-AGAO, but the equilibrium strongly favors TPQ_{amr} such that TPQ_{sq} forms in undetectable levels. This could also explain why the oxidative half-reaction is so much slower in these systems. Our data cannot discount this possibility.

(62) Kumar, V.; Dooley, D. M.; Freeman, H. C.; Guss, J. M.; Harvey, I.; McGuirl, M. A.; Wilce, M. C. J.; Zubak, V. M. *Structure* **1996**, *4*, 943−955.

(63) Kyte, J. *Mechanism in Protein Chemistry*; Garland Publishing: New York & London, 1995.

(64) Zhang, L.; Bandy, B.; Davison, A. J. *Free Radical Biol. Med.* **1996**, *20*, 495−505.

The hydrogen-bonding network around the active site involving metal-coordinating and noncoordinating water molecules is essentially the same among Cu-, Co-, and Ni-AGAO with very similar hydrogen bond distances (Figure 7c,d). Further, in the Co- and Ni-AGAO structures, there is no residue whose side chain takes a position considerably different from that in the Cu-AGAO structure and thereby could be relevant to the decreased activity of the metal-substituted enzymes (including TPQ382 and Tyr284; see Figure 8a). Therefore, if the reduced dioxygen species were bound to the axial position of the metal ion in Co- and Ni-AGAO, as in Cu-AGAO, where the similar hydrogen-bonding network would be formed and serve as the proton-transfer pathway in the conversion of TPQ_{sq2} to TPQ_{imq}, then the low activities of Co- and Ni-AGAO should be finally ascribed to the intrinsic properties of the metal ion itself.

The Lewis acidity of metal ions influences acid dissociation constants of metal-bound water, Cu^{2+} lowering the pK_a by ~2 pH units as compared to Co^{2+} and Ni^{2+}.[65,66] It is possible that these differences in Lewis acidity may affect the efficiency of the oxidative half-reaction. However, the pK_a-lowering effect would rather be disadvantageous for the formation and subsequent release of the metal-bound reduced dioxygen species, as they have to be protonated. This trend is moderated as the reduced dioxygen species are only weakly bound to Cu^{2+} as an axial ligand, so, while still being stabilized (localized), they are not made unduly acidic, thereby hindering protonation. In this study, we conclude that the relative Lewis acidities of the metal ions are not controlling the rate of electron- or proton-transfer reactions in the oxidative half-reaction. Rather, the rate-limiting step in the oxidative half-reaction of Co- and Ni-AGAO is the net $2e^-$-electron transfer from TPQ_{amr} to dioxygen, where it is possible that the rate acceleration seen in Cu^{2+} is due to the disproportionation reaction, which forms Cu^{1+} and TPQ_{sq2}, and the ability of Cu to bind reduced O_2 species in a facile manner.

Concluding Remarks

The present results obtained with the metal-substituted enzymes of a bacterial CAO contrast with those obtained with eukaryotic CAOs, in particular, HPAO,[14] in a number of aspects that should be noted: (i) In the oxidation of TPQ_{sq}/TPQ_{amr} to TPQ_{ox}, Zn^{2+} is almost inactive for AGAO, while it is significantly active (even more active than Co^{2+}) for HPAO. (ii) Although Co^{2+} is the second best metal ion following the native Cu^{2+} for the activities of both AGAO and HPAO, the recovered specific activities relative to that of the native Cu-enzyme are considerably different (19% in HPAO, 2.2% in AGAO). (iii) Most importantly, the major cause for the reduced activities of the metal-substituted enzymes is the marked increase in K_m for O_2 in Co-HPAO, whereas it is the marked drop of k_{cat} in Co- and Ni-AGAO with little changes in K_m values for substrate amine and dioxygen. The reason for the difference observed between AGAO and HPAO is unclear at this stage.

Our results show that the rate-limiting step in the catalytic cycle of the metal-substituted AGAO is in the oxidative half-reaction. In Co- and Ni-AGAO, this rate-limiting step is most likely the reaction between TPQ_{amr} and dioxygen. Under the single turnover conditions, the rate-limiting step is the hydrolysis of TPQ_{imq} to TPQ_{ox} similar to what was observed for Cu-AGAO. While our results are consistent with the proposed role of the metal ion in promoting the reduction of superoxide in eukaryotic CAOs,[13,14] we cannot rule out the possibility that Cu^{2+} changes its valence state prior to the oxidation of TPQ_{amr}. Future studies of, in particular, the structures of both the reduced and the TPQ_{imq} forms of Co- and Ni-AGAO, will help further elucidate the role of Cu^{2+} in the catalytic cycle of AGAO.

Acknowledgment. We thank Dr. Julian Limburg and Dr. Hideyuki Hayashi for critical reading of the manuscript and helpful discussions. We also thank the National Institute of Genetics (Mishima, Japan) and Kyowa Hakko Kogyo (Tokyo, Japan) for providing the catalase-deficient mutants of *E. coli*. This work was supported by Grants-in-aid for Scientific Research (B: 12480180), Priority Area (B: 13125204), "Research for the Future", and an Osaka University Center of Excellence (COE) program "Creation of Highly Harmonized Functional Materials" from the Japan Society for the Promotion of Science.

Note Added after ASAP: The version of this paper published on the Web 1/4/2003 did not include the caption to Figure 7. The final Web version published 1/7/2003 and the print version are correct.

JA017899K

(65) Huheey, J. E. *Inorganic Chemistry, Principles of Structure and Reactivity*; Harper & Row: New York, 1972; p 214.
(66) Margerum, D. W.; Cayley, G. R.; Weatherburn, D. C.; Pagenkopf, G. K. In *Coordination Chemistry*; Martell, A. E., Ed.; ACS Monograph 174; American Chemical Society: Washington, DC, 1978; Vol. 2, pp 1−220.